Tellus (2008), 60B, 432–469
Printed in Singapore. All rights reserved

TELLUS

Hygroscopic properties of submicrometer atmospheric aerosol particles measured with H-TDMA instruments in various environments—a review

By E. SWIETLICKI[1]*, H.-C. HANSSON[2], K. HÄMERI[3], B. SVENNINGSSON[4], A. MASSLING[5], G. MCFIGGANS[6], P. H. MCMURRY [7], T. PETÄJÄ[3,8], P. TUNVED[2], M. GYSEL[9], D. TOPPING[6,10], E. WEINGARTNER[9], U. BALTENSPERGER[9], J. RISSLER[1], A. WIEDENSOHLER[5] and M. KULMALA[3], [1]*Division of Nuclear Physics, Lund University, PO Box 118, S-22100 Lund, Sweden;* [2]*Department of Applied Environmental Science, Stockholm University, S-10691 Stockholm, Sweden;* [3]*Division of Atmospheric Sciences, PO Box 64, FI-00014 University of Helsinki, Finland;* [4]*Department of Physical Geography and Ecosystems Analysis, Lund Univ., PO Box 118, S-221 00 Lund, Sweden;* [5]*Department of Physics, Leibniz-Institute for Tropospheric Research, D-04318 Leipzig, Germany;* [6]*Atmospheric Sciences Group, SEAES, Univ. of Manchester, Oxford Road, Manchester, M13 9PL, UK;* [7]*University Minnesota, Department of Mechanical Engineering, 111 Church St SE, Minneapolis, MN 55455, USA;* [8]*Earth and Sun Systems Laboratory, Atmospheric Chemistry Division, National Center for Atmospheric Research, PO Box 3000, Boulder, CO 80307-5000, USA;* [9]*Laboratory of Atmospheric Chemistry, Paul Scherrer Institut, 5232, Villigen PSI, Switzerland;* [10]*NCAS, SEAES, University of Manchester, Oxford Road, Manchester, M13 9PL, UK*

(Manuscript received 16 November 2007; in final form 29 February 2008)

ABSTRACT

The hygroscopic properties play a vital role for the direct and indirect effects of aerosols on climate, as well as the health effects of particulate matter (PM) by modifying the deposition pattern of inhaled particles in the humid human respiratory tract. Hygroscopic Tandem Differential Mobility Analyzer (H-TDMA) instruments have been used in field campaigns in various environments globally over the last 25 yr to determine the water uptake on submicrometre particles at subsaturated conditions. These investigations have yielded valuable and comprehensive information regarding the particle hygroscopic properties of the atmospheric aerosol, including state of mixing. These properties determine the equilibrium particle size at ambient relative humidities and have successfully been used to calculate the activation of particles at water vapour supersaturation. This paper summarizes the existing published H-TDMA results on the size-resolved submicrometre aerosol particle hygroscopic properties obtained from ground-based measurements at multiple marine, rural, urban and free tropospheric measurement sites. The data is classified into groups of hygroscopic growth indicating the external mixture, and providing clues to the sources and processes controlling the aerosol. An evaluation is given on how different chemical and physical properties affect the hygroscopic growth.

1. Introduction

Aerosol particles affect the radiation balance of the atmosphere in a number of ways. They scatter and absorb incoming shortwave radiation and absorb outgoing long-wave radiation (the 'direct aerosol climate effect'). Aerosol particles that act as cloud condensation nuclei cause changes in droplet number affecting the albedo and persistence of clouds; the latest IPCC report refer to these respectively as the cloud albedo and the cloud lifetime aerosol indirect climate effects (Randall et al., 2007). The hygroscopic properties of atmospheric aerosol particles are vital for a proper description of these effects, since they describe how the particles interact with water vapour both at sub and supersaturated conditions (e.g. McFiggans et al., 2006). They are thus of major importance in describing the life cycle of the aerosol and the related direct and indirect effects on climate.

The hygroscopic properties can be measured in great detail using Hygroscopic Tandem Differential Mobility Analyzers instruments (H-TDMA). Based on the pioneering work of Liu et al. (1978) a wide variety of designs exist, which are described

*Corresponding author.
e-mail: Erik.Swietlicki@nuclear.lu.se
DOI: 10.1111/j.1600-0889.2008.00350.x

in more detail in Section 2. However, all systems use the same principle to extract a narrow size cut from a polydisperse aerosol, expose this to a well defined enhanced relative humidity (RH) and determine the increase of the particle diameter due to the water uptake at this enhanced RH.

The description of the equilibrium size of a droplet with water saturation ratio, founded on the early work of (Köhler, 1936), is now well established and can be readily derived from the Clausius–Clapeyron equation modified to give a general equilibrium relation between 'an aqueous solution droplet and water vapour:

$$\frac{e}{e_s} = a_{\mathrm{w}} C_{Ke} = a_{\mathrm{w}} \exp\left(\frac{2 v_{\mathrm{w}} \sigma_{\mathrm{sol}/v}}{RTr}\right), \tag{1}$$

where e is the vapour pressure of water, e_{s} is the saturation vapour pressure of water, $e/e_{\mathrm{s}} = S$, is known as the saturation ratio, or relative humidity, RH, a_{w} is the water activity, C_{Ke} is the Kelvin curvature correction factor, v_{w} is the partial molar volume of water, $\sigma_{\mathrm{sol}/v}$ is the surface tension of the solution at the composition of the droplet, R is the universal gas constant, T is the temperature and r is the equilibrium radius.

The Köhler equation states that the saturation ratio, or relative humidity RH, equals the water activity for a plane solution surface, and that for curved surfaces such as aerosol particles, the water activity is always smaller than the ambient RH. The Kelvin factor therefore causes the diameter growth due to water uptake to decrease with decreasing dry size for particles of identical composition. The influence of the surface tension appearing in the Kelvin factor is however small at subsaturated conditions. Water-soluble aerosol particles grow by condensation of water vapour simply because the water activity of the aqueous solution strives to equilibrate to the RH in the surrounding air in accordance with the Köhler equation.

This work first reviews and summarizes the existing H-TDMA data sets as well as potential error sources and inversion algorithms. The major part of the paper then focuses on H-TDMA data, with an emphasis on those published so far in peer-reviewed journals. The aim is to present the data in a way that will make it useful in evaluating models on various spatial and temporal scales incorporating a more detailed aerosol description than simply aerosol mass. To facilitate comparison between sites, growth factors are recalculated to an RH of 90%, and classified according to the air mass properties and geographical location.

2. H-TDMA instruments

2.1. H-TDMA principle of operation

The Tandem Differential Mobility Analyzer technique (TDMA) was first introduced by Liu et al. (1978) as a technique to study the change in particle diameter (more precisely electrical mobility) as a result of an imposed aerosol processing. They referred to this system as the aerosol mobility chromatograph. Rader and McMurry (1986) introduced the 'TDMA' terminology, and showed that data could be inverted to enable measurements of size changes as small as 1% (less than 1 nm for particles smaller than 100 nm). TDMAs have been used to study size changes associated with humidification (H-TDMA), evaporation (V-TDMA), chemical reactions (R-TDMA) and uptake of organic vapours (O-TDMA). In the H-TDMA (Hygroscopic Tandem Differential Mobility Analyzer) instrument (Sekigawa, 1983; McMurry and Stolzenburg, 1989), the aerosol particles are processed by humidification. The aim of H-TDMA measurements is to obtain the distribution of growth factors (*Gf*) exhibited by the particles of the selected dry size upon exposure to high RH, hereinafter referred to as the growth factor probability density function (*Gf*-PDF). The hygroscopic growth factor *Gf* is the ratio between humidified (d_{w}) and dry particle diameter (d_{d}) at a well-defined relative humidity RH.

$$G_f = \frac{d_{\mathrm{w}}}{d_{\mathrm{d}}}. \tag{2}$$

Often only integral properties of the *Gf*-PDF are reported, including proportions of particles in separated modes of the *Gf*-PDF (e.g., 'more' and 'less' hygroscopic particles), or mean mobility diameter growth factor and variability in growth factors for each mode.

The H-TDMA is thus capable of quantifying the changes in the aerosol particle electrical mobility diameter induced when taking the particles from a 'dehydrated' reference state to an environment where they are exposed to an elevated relative humidity. The increase in particle diameter (and thus also particle volume) is postulated to be caused entirely by condensation of water vapour, which in turn is assumed to be controlled by a thermodynamic equilibrium between the condensed water and the surrounding water vapour. In most cases, the assumption of equilibrium conditions provides an adequate approximation of the particle diameter changes, as can be verified by studying reference compounds, or by means of so called hygroscopicity closure studies. Various theories and models describing this thermodynamic equilibrium can thus be used to predict water activities and water uptake as a function of particle chemical composition (Section 5).

Similar to the H-TDMA, the electrodynamic balance (EDB; Peng and Chan, 2001, and references therein) is also capable of measuring the equilibrium between condensed water and water vapour for individual aerosol particles (or the water activity of the solution). The EDB, however, relies on the balancing of the gravitational force by an alternating electrical field and is typically used for particles larger than a few micrometres in diameter. Since only one single particle can be suspended at a time, and this particle needs to be trapped in the EDB for minutes or longer, this technique is not suitable for studies of hygroscopic growth of atmospheric aerosol particles. Contrary to the EDB, the H-TDMA instrument is a genuine flow-through system, capable of delivering data on the distribution of hygroscopic diameter

growth for a large number of submicrometre aerosol particles for each particle dry diameter and RH. The H-TDMA is therefore well suited for field studies of the hygroscopic properties of atmospheric aerosol particles.

EDB instruments have nevertheless produced valuable water activity data in numerous laboratory studies of both inorganic salts and water-soluble organic compounds (Kanakidou et al., 2005). These laboratory EDB measurements can be directly incorporated into thermodynamic models and mixing rules describing the hygroscopic properties because those models often express water uptake on a mole fraction basis. Such data have been used extensively to validate the performance of H-TDMA instruments. The two instruments also give complementary data as the EDB provides information about mass increase due to water uptake and the H-TDMA data represent diameter (volume) changes. A combination of both will thus give information about effective density.

H-TDMA instruments consist of two Differential Mobility Analyzers (DMAs), an aerosol drier, an aerosol bipolar charger, humidifiers for the aerosol and sheath flows, and a particle counter (Fig. 1). The aerosol drier is generally the first component of the H-TDMA downstream the aerosol inlet, and serves to ensure that the particles are dehydrated before entering the bipolar charger and classification of particle dry size in the first DMA. Here, 'dry' aerosol particles are selected in a narrow quasi-monodisperse size interval. These size-classified particles are subsequently humidified in an aerosol humidifier and led to a second DMA where the new, humidified particle size distribution is determined (Fig. 2). Condensation particle counters (CPC) are typically used to determine the particle number concentrations in the aerosol outlet flows from the DMAs. Since every individual particle is counted, H-TDMA measurements can be carried out even in very clean environments such as the central Arctic Ocean (Zhou et al., 2001).

Several dry particle sizes, d_d, are examined in most H-TDMA studies. Inclusion of at least one dry size in the centre of the Aitken (~50 nm) and accumulation mode (~150 nm) should be considered a minimum. Several studies have extended the set of dry sizes to cover a wider range to enable a more complete description of $Gf(\mathrm{RH},d_d)$, for instance $d_d = 35$, 50, 75, 110, 165 and 265 nm.

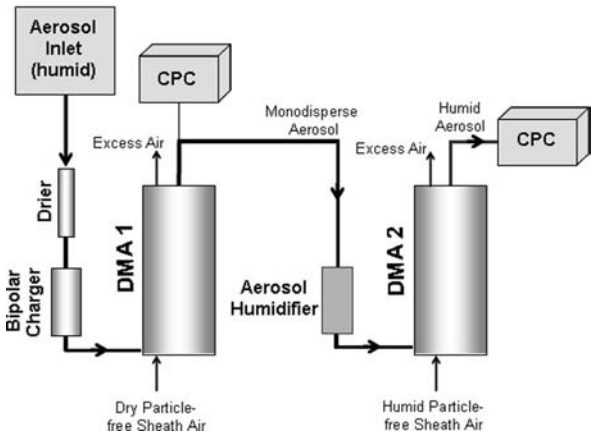

Fig. 1. Shematic picture of an H-TDMA instrument. CPC: Condensation Particle Counter; DMA: Differential Mobility Analyzer.

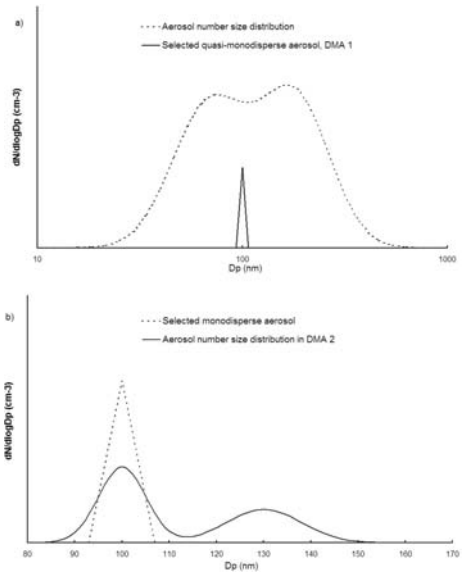

Fig. 2. The working principle of the H-TDMA. DMA1 selects 'dry' aerosol particles in a narrow quasi-monodisperse size interval (a). These size-classified particles are subsequently humidified in an aerosol humidifier and led to DMA2 where the new, humidified particle size distribution is determined (b).

For each dry size, DMA2 is scanned over a size range corresponding to hygroscopic growth factors between $Gf = 0.9$–2.0 or slightly larger (at RH = 90%). The DMA2 scan range may differ from one dry size to the other, and depends on the properties of the actual aerosol being studied. To capture all externally mixed sea salt particles in DMA2, the scan range often needs to be extended to $Gf = 2.5$. It should, at all times during an experiment, be ascertained that all humidified particle sizes are covered in full.

Depending on the number of DMA1 dry sizes, DMA2 growth factor scan ranges and CPC2 counting statistics, the time resolution in most H-TDMA field measurements are between 0.5 and 1 h. This means that each dry size is scanned (in DMA2) once during this time period.

The RH to which the particles are subjected can be varied over a wide range (~5% to ~99%), and the H-TDMA can thus be used to study the full RH hysteresis behaviour of atmospheric aerosol particles.

The majority of H-TDMA instruments operate at temperatures around 20–25 °C. Weingartner et al. (2002) developed a low-temperature H-TDMA system to avoid volatilization of semi-volatile material during measurements at subfreezing temperatures at a high alpine site.

At present, there are no commercially available H-TDMA instruments, and all existing instruments are constructed and operated by the various aerosol research groups. The specific designs therefore vary between instruments, although the working principle and main parts are common to all H-TDMA instruments. In particular, H-TDMA users have chosen different solutions for the humidity control of the quasi-monodisperse aerosol and the particle-free sheath air entering the second DMA.

The primary parameters measured with an H-TDMA as a function of dry particle diameter, and derived from the *Gf*-PDF, are (i) the hygroscopic growth factor (*Gf*); (ii) the number fraction (*AF*) of particles belonging to each of the observed and separable groups of hygroscopic growth and (iii) the spread of diameter growth factors around the arithmetic mean *Gf* value (σ_{Gf}). Alternatively, the H-TDMA measurements can also be presented as distributions of hygroscopic growth factors for each given dry particle diameter (representations of *Gf*-PDF).

An aerosol is said to be externally mixed when particles of a given (dry) size have different chemical composition. In a perfect internal mixture, all particles have identical composition. The H-TDMA is one of very few aerosol instruments capable of providing on-line and in situ information regarding the extent of external versus internal mixing of the atmospheric aerosol, since the H-TDMA determines the hygroscopic growth of individual aerosol particles. The H-TDMA instrument separates particles (of a particular dry size) into groups of similar hygroscopic properties (water uptake). Although this state of mixing strictly refers only to the hygroscopic properties, it nevertheless implies the extent of chemical mixing of the aerosol. However, it needs to be pointed out that externally mixed particles of similar hygroscopic growth cannot be separated using H-TDMA instruments.

2.2. TDMA data inversion

As already described, TDMA measurements involve selecting particles of a given mobility size with DMA1, processing those particles in an 'aerosol conditioner,' and measuring the concentration of those particles (N2) downstream of DMA2 with a condensation particle counter for a sequence of DMA2 classifying voltages (V2). In H-TDMA systems, aerosol conditioning involves adjusting the relative humidity of the sampled aerosol, which leads to size changes for hygroscopic particles. The dependence of concentration on voltage, N2(V2), is obtained by stepping or scanning DMA2.

N2(V2) is then analyzed to obtain information on the *Gf*-PDF. However, N2(V2) is only a smoothed and skewed image of the *Gf*-PDF because the DMA's transfer function has a finite width and because the total transfer probability depends on V2, respectively. Mean diameter growth factors and relative proportions of particles in separated groups derived from N2(V2) are generally biased, except for samples exhibiting uniform growth with little spread. Only coarse information on the variability of behaviour for particles of a given type is obtained from N2(V2) because of the smoothing. Therefore a data inversion algorithm is required to derive the key properties of the *Gf*-PDF from N2(V2) accurately.

One class of approaches to invert TDMA data takes the Kernel function of the full TDMA system into account, thus retrieving the true *Gf*-PDF as close as possible within the limitations imposed by the inversion algorithm and the measurement uncertainties. The TDMAFit algorithm developed by Stolzenburg and McMurry (1988) allows for the existence of multiple groups of particles with distinctly different hygroscopic behaviour. The groups in the *Gf*-PDF are assumed to follow a normal distribution (Gaussian shape) with variable standard deviation, thus allowing for the possibility that particles of a given type are not all identical, but rather grow to varying extents due to small differences in composition. The only disadvantage of this approach is that convergence of fitting multiple groups is not very robust for nearby, overlapping groups. Furthermore, determining whether or not groups can be resolved is subjective. Cubison et al. (2005) adapted the optimal estimation method of Rodgers (1976, 1990) to H-TDMA data inversion. This approach uses a quasi-inverse matrix of the TDMA kernel function in order to retrieve the values of the *Gf*-PDF at discrete bin positions. This method returns unambiguous results for given retrieval bins and objectively determines the minimum group separation that can be resolved, while it is less effective at evaluating the growth spread factor for particles of a given type. Gysel et al. (2007) developed an inversion algorithm, which represents the inverted *Gf*-PDF as a piecewise linear function. This algorithm provides equivalent information to TDMAfit, with the advantage that convergence of the inversion is robust and independent of the initial guess, even for complex asymmetric and multimodal *Gf*-PDFs. In addition this method objectively determines the minimum group separation that can be resolved.

In an alternative class of approaches, only the sizing done with DMA2 is inverted in order to retrieve the *Gf*-PDF. In doing so it is crucial to account for the narrow size distribution entering DMA2. DMA inversion algorithms that properly invert narrow size distributions have been developed by, for example, Stratmann et al. (1997) and Voutilainen et al. (2000). A *Gf*-PDF obtained in this way is somewhat smoothed compared to the true *Gf*-PDF because the size cut selected by DMA1 is not perfectly monodisperse. The mean diameter growth factors and relative proportions of particles in separated groups are accurately determined, while the smoothing has a small effect on the growth dispersion within a group.

Some investigators have applied SMPS (Scanning Mobility Particle Sizer) data analysis methods (e.g. Wang and Flagan, 1990) to invert N2(V2) data from TDMA systems. However, SMPS methods assume that the mobility distribution entering DMA2 is invariant across the DMA2 mobility window and they include corrections for charging probability, both of which are never valid for TDMA measurements (Rader and McMurry,

1986). Therefore SMPS methods can only be used to obtain N2(V2) by exporting the data in the unit 'raw counts', thus strongly restricting data interpretation as described above.

To date, analyses of H-TDMA data have focused on determining mobility diameter growth factors and the relative proportions of different particle types. While H-TDMA data may include information on the variability in water uptake for particles of a given type, such information has not yet been systematically explored.

2.3. H-TDMA sources of error

2.3.1. Errors caused by RH and temperature variability. Correct H-TDMA *Gf* measurements hinge upon accurate RH control in DMA2. The RH should be constant over the entire DMA, from the aerosol entrance slit inside the DMA to the aerosol outlet slit. The aerosol particles should also have time to equilibrate to the high RH before entering DMA2. These criteria will ensure that the particles remain at a constant size during transit through the DMA2 column. Since RH is highly dependent on temperature at these high humidities, it is essential that temperature gradients inside DMA2 are also minimized.

The most efficient way to reduce temperature variations is to encapsulate the entire DMA2 and its connections in a closed and well insulated container filled with either air (Swietlicki et al., 2000; Massling et al., 2005) or some liquid (Weingartner et al., 2002; Hennig et al., 2005). The best solution is to actively control the temperature of the container, and not merely to insulate it thermally from the laboratory environment. The particle-free DMA2 sheath air also needs to be controlled to the same temperature, for instance using efficient heat exchangers. To ensure that the DMA2 RH is accurate to within $90 \pm 1\%$ RH, the temperature should not vary more than $\sim \pm 0.2\ ^{\circ}$C. This also happens to be close to the accuracy and precision of many commonly used temperature sensors. The RH performance of H-TDMA instruments therefore needs to be checked regularly by means of an independent measurement. Most systems use particles of pure salts, such as ammonium sulphate, to ensure that the measured *Gf* corresponds to the expected value (Chan and Chan, 2005). Such quality checks should be performed regularly during H-TDMA field operation, preferably on daily basis. The deliquescence behaviour of pure salts has also often been used to determine the RH accuracy and precision. The reference salt solutions need also to be freshly mixed in order to exclude bacterial activity from modifying the solution properties.

Table 2 in Chan and Chan (2005) summarizes the information available as of 2005 on the reference salts that were used for H-TDMA system quality assurance in various field studies. With one exception (KCl), only ammonium sulphate and NaCl salts were used. A note of caution; most nebulizers generating NaCl particles from a solution produce non-spherical particles with a shape factor that may be larger than unity, and even approaching that of a perfect cube (1.08) (Hameri et al., 2001a; Gysel et al., 2002; Biskos et al., 2006). This may cause an underestimation of the measured growth factor, which is undesirable when used as a reference. For this reason, ammonium sulphate is a better choice, or the combination of both salts.

An H-TDMA system with accurate DMA2 RH control—implying active DMA2 temperature control—should be able to produce reliable *Gf* distributions that require no further off-line corrections for RH. In practice, small corrections of the measured *Gf* value from the actual to the nominal RH (for instance 90%) are often needed to ensure data intercomparability (Swietlicki et al., 1999).

In other systems, in particular those with passive DMA2 temperature control systems, the actual DMA2 RH may deviate significantly from the nominal value. These H-TDMA systems can still produce sound *Gf* data provided that the temporal variability of the DMA2 RH can be reproduced with sufficient accuracy (Rissler et al., 2006). A chilled-mirror dew point hygrometer can be used to measure the excess air dew point temperature, which is also assumed to be identical to the dew point temperature inside DMA2, to within $\pm 0.1\ ^{\circ}$C. The temperature of the air flowing inside DMA2 then remains to be known in order to calculate the DMA2 RH. This temperature is often difficult to measure directly and often has to be estimated from temperatures in other parts of the system. The validity of this temperature estimate (and thus also the DMA2 RH estimate) needs to be checked against *Gf* measurements on pure salt particles.

Whatever strategy is used, the quality assurance procedure should be clearly stated in any H-TDMA publication, which has not always been the case. Otherwise, one might suspect that the *Gf* errors may be substantially higher than those stated by the authors.

2.3.2. Errors caused by the DMA electrical mobility classification. Since the DMA classifies particles according to their electrical mobility, several factors may influence the accuracy of the measured *Gf* values. The shape of the humidified particle is almost invariably that of a perfect sphere (shape factor $\chi = 1$). The DMA2 will therefore provide an accurate measurement of the (singly charged) particle diameter. The dry particles may, however, have shape factors that significantly deviate from unity. This may cause the measured *Gf* values to be lower than expected from the volume and nature of the soluble material present in the dry particle. For highly agglomerated aerosols, such as fresh combustion aerosols, this effect could be quite severe (Rissler et al., 2005). A way around this problem is to pre-process the aerosol to make the particles more spherical, for instance by pre-humidification and subsequent drying before entering the first DMA. This is not needed in atmospheric H-TDMA measurements unless these are performed in the immediate vicinity of a strong particle source. This potential source of error could also be turned to an advantage and used to estimate the fractal dimension (or shape factor) for agglomerated aerosols (Rissler et al., 2005).

Another potential problem relating to the sizing of the particles in DMA1 is the possibility that they may actually not be perfectly dehydrated at the prevailing DMA1 RH. Particles containing some compounds may escape efflorescence and retain small amounts of particle-bound water when dried. Sulphuric acid is a classic example, but the same may be true for common atmospheric salts such as ammonium bisulphate and ammonium nitrate (Mikhailov et al., 2004; Svenningsson et al., 2006a), and mixtures of organic compounds (Marcolli et al., 2004). For this reason, it is desirable to maintain the DMA1 RH as low as possible, at least <15% RH. The ambient aerosol should also be dried before entering DMA1, preferably also before charging, in order to minimize the number fraction of multiply charged particles. The unknown shape and phase of the particles in DMA1 should be considered as a potential source of error in laboratory experiments and closure studies.

In principle, it would be possible to correct for multiple charges in the TDMA inversion algorithm. The multiple charge correction requires knowledge of the (dry) aerosol size distribution from the smallest DMA1 dry size to at least twice the largest dry size. The H-TDMA instrument itself could be used to generate such data, and if not, parallel size distribution measurements using a Differential (or Scanning) Mobility Particle Sizer (DMPS or SMPS) are required. As far as we are aware, H-TDMA multiple charge correction has never been done for atmospheric aerosols. The error introduced by ignoring multiple charges is probably small in most cases, since the H-TDMA operates in a size interval where the fraction of multiple charged particles is fairly small (dry sizes < 400 nm). Furthermore, observed atmospheric *Gf* values typically vary rather little between diameters corresponding to singly and doubly charged particles for a given DMA1 electrical mobility. An impactor may also be placed between the aerosol drier and DMA1 to at least eliminate the supermicrometre sized particles. However, care should be taken when selecting the impactor cut-off diameter since the conversion from equivalent aerodynamic to mobility diameters depends on particle density, which is often unknown for atmospheric aerosols. Nevertheless, multiple charges might be of importance when examining the hygroscopic properties of particles with sizes below the number median diameter of a narrow size distribution, which is often the case in laboratory studies. We therefore recommend that the effect of multiple charges on the measured *Gf* values should be investigated further.

2.3.3. Errors caused by particle non-equilibrium conditions in DMA2. A basic assumption in H-TDMA measurements is that the particles in DMA2 are observed when in equilibrium with the surrounding water vapour. While this is correct for nearly all inorganic salt particles, Chan and Chan (2005) and Kerminen (1997) have pointed out that this is not necessarily true for all atmospheric particles, especially for some organic compounds, very viscous particles, and particles with low accommodation coefficients. Residence times of a few seconds at the elevated DMA2 RH or slightly below [as is typically the case in most H-TDMA systems; Table 2 in Chan and Chan (2005)] may not be enough for such particles to attain their equilibrium humidified size (Sjogren et al., 2007b). This was also observed to be the case for a small number fraction (<3%) of particles in a study in Mexico city (Chuang, 2003). More references on this subject are given in Chan and Chan (2005), who also recommended that the residence time for humidification in H-TDMA studies should be reported.

Evaporation losses of volatile compounds between DMA1 and DMA2, for instance for ammonium nitrate particles, may also cause problems in H-TDMA measurements. It is difficult to estimate the influence that evaporation may have had on reported atmospheric *Gf* values.

2.3.4. Conclusions regarding the accuracy of the published H-TDMA data. Considering the possible sources of error in H-TDMA field measurements, it is relevant to ask how reliable the existing data actually are. Are the data intercomparable? Can they be used as input data for closure studies? We will limit our discussion to the reliability of the most important primary parameter derived from the *Gf*-PDF, namely the hygroscopic growth factor (*Gf*).

Since ammonium sulphate is often used as reference salt to estimate the soluble volume fraction (ε_{AS}) of the dry particles (see Section 3.2), we use this salt to illustrate the *Gf* accuracy. Figure 3 shows the requirements for DMA2 RH accuracy and stability in order to maintain the errors in *Gf* to within ±0.02 and 0.05 of the reported *Gf* value, for ε_{AS} ranging from 0.1 to 1.0. For a 100 nm dry size particle with $\varepsilon_{AS} = 1.0$ (pure ammonium sulphate), DMA2 RH fluctuations or inaccuracies between 88.6 and 91.2% RH will result in a variability in *Gf* of ±0.05 around the correct value of $Gf = 1.70$. This corresponds to a variability in DMA2 temperature of $\sim \pm 0.2$ °C. In order to achieve a combined accuracy and precision in *Gf* of ±0.02, then the DMA2 RH needs to be controlled to between 89.5 and 90.5%, with a corresponding DMA2 temperature variability better than ±0.1 °C. This is not achieved in most H-TDMA field measurements.

The requirements for RH and temperature stability are somewhat less stringent at lower soluble volume fractions. For a 100 nm dry size particle with $\varepsilon_{AS} = 0.3$, a *Gf* error of ±0.02 (around the correct value of $Gf = 1.29$) can be obtained even when the DMA2 RH varies between 90 ± 1%.

The conclusion is that, in H-TDMA systems capable of controlling the DMA2 RH to within ±0.2 °C during field measurements, the error in the measured *Gf* at RH = 90% can be within ±0.05 for particle in the more-hygroscopic group. The same variability in RH and temperature will result in a *Gf* error within ±0.02 for particles in the less-hygroscopic group. This can only be achieved if the DMA2 RH and temperature is closely monitored and controlled, and if the performance of the H-TDMA system is regularly checked by means of reference salts. Since these are standard procedures for all H-TDMA field instruments, we conclude that the reported *Gf* values are reliable to within ±0.05.

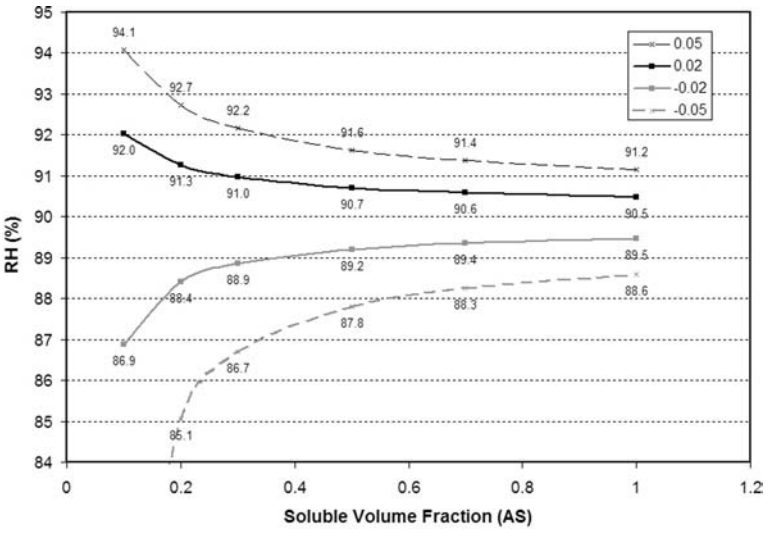

Fig. 3. The effect of variability in RH on the measured *Gf* value for ammonium sulphate particles with 100 nm dry size. The figures shows the RH required in order to limit the *Gf* value to stay within ±0.05 and ±0.02 of the correct value for a range of soluble volume fractions (AS: ammonium sulphate used as model reference salt)

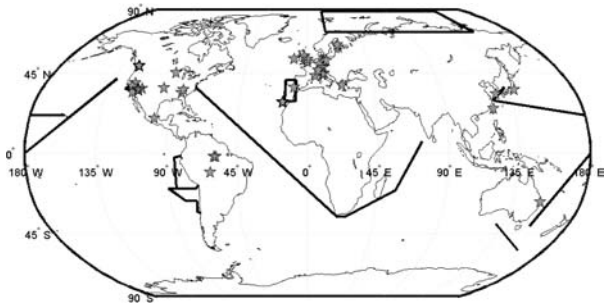

Fig. 4. Global map showing locations of H-TDMA experiments.

3. H-TDMA measurements

3.1. H-TDMA data compilations

Compilations of H-TDMA data on atmospheric aerosols have been presented previously (Cocker et al., 2001; Chan and Chan, 2005; Kanakidou et al., 2005; McFiggans et al., 2006; Kandler and Schutz, 2007). These were focusing on specific topics related to hygroscopicity, such as urban aerosols (Cocker et al., 2001), modelling organic aerosols (Kanakidou et al., 2005), mass transfer limitations (Chan and Chan, 2005), CCN properties (McFiggans et al., 2006) and solubility (Kandler and Schutz, 2007). Here, we attempt to provide a more comprehensive overview in the sense that we include all H-TDMA data on atmospheric aerosols reported up to September 2007, and draw conclusions regarding the characteristic hygroscopic behaviour of aerosol particles in various environments (marine, rural, urban, free tropospheric) and for nucleation mode particles. We classify the H-TDMA data into commonly observed groups of hygroscopic growth to facilitate data classification and comparability. We also identify H-TDMA measurement errors, and discuss the current status of models calculating water uptake from chemical composition.

3.2. Data classification

Over the last 25 yr, H-TDMA instruments have been used in several field measurements to study the hygroscopic properties of submicrometre atmospheric aerosol particles at various sites around the globe (Fig. 4). The sites include remote marine and coastal environments (Atlantic Ocean, Pacific Ocean, Indian Ocean, Arctic Ocean), background continental sites (Amazon rain forest, Nordic boreal forest, the Alps, North America), polluted continental sites (Italy, United Kingdom and Germany), and polluted urban sites (Germany, North America, Mexico and Asia). Air masses influenced by fresh as well as aged biomass burning have been studied in North and South America. Atmospheric new particle formation events have been observed frequently in several locations over the globe. The existing H-TDMA data on atmospheric aerosols are nearly all from short intensive field campaigns covering time periods of a few weeks to maximum 8 months (Massling et al., 2005, urban study). We are not aware of any real long-term H-TDMA data sets (>8 months). The geographical data coverage is also limited with notable deficiencies, in particular in Africa and Asia.

The H-TDMA field data are complemented by studies of the hygroscopic properties of aerosol particles emitted from various sources, such as fresh diesel vehicle exhaust and flue gases from biomass combustion. Secondary organic aerosols have also been investigated in a variety of smog chamber experiments. These data, and laboratory water activity data, will only be discussed here for the purpose of interpreting the field H-TDMA observations. A compilation of H-TDMA laboratory studies involving water-soluble organic compounds is found in Kanakidou et al. (2005).

The hygroscopic properties of ambient aerosol particles vary strongly depending on the origin of the air masses and the location. In continental, polluted air masses the aerosol is often separated into two groups traditionally denoted as being less- and

more-hygroscopic particles. At high wind speeds, remote marine aerosols typically show an external mixture with a ubiquitous sulphate-rich more-hygroscopic particle group and a sea-salt group displaying even higher hygroscopic growth. In urban air, nearly hydrophobic particles originating from combustion are observed in mixtures with long-range transported background aerosol particles that are less- and more-hygroscopic.

Owing to these frequent observations of externally mixed aerosols, the H-TDMA data is often presented as averages of the hygroscopic growth factor (*Gf*) and the number fraction (*AF*) for each group of hygroscopic growth. In addition, some studies report also the spread of diameter growth factors around the average *Gf*, frequency of occurrence of each hygroscopic group, and frequency of occurrence of external mixtures. The presentations of H-TDMA data are not entirely consistent and directly comparable, in particular regarding number fractions and frequencies of occurrence.

Here, we adhere to the traditional nomenclature aiming to describe the various particle groups of hygroscopic growth. The available field H-TDMA data is thus separated into nearly hydrophobic particles, less-hygroscopic particles, more-hygroscopic particles, and finally sea-salt particles. This covers the entire range of observed *Gf* ranging from $Gf \approx 1$–2.3 (at RH = 90%).

Since the Kelvin curvature correction results in decreasing *Gf* for decreasing particle size (for particles of identical chemical composition and dehydrated shape), the classification of *Gf* data is more consistent when this curvature effect is taken into account. A straight-forward and often used way to do this is to apply the concept of soluble particle volume fraction, ε (Svenningsson et al., 1994; Swietlicki et al., 1999). The soluble volume fraction ε can also be considered a proxy for the chemical composition. A reference compound or chemical composition has to be used when calculating ε from H-TDMA data. For ammonium sulphate, $\varepsilon_{\mathrm{AS}}$ is calculated according to

$$\varepsilon_{\mathrm{AS}} = \frac{Gf^3 - 1}{Gf_{\mathrm{AS}}^3 - 1}. \quad (3)$$

Here, *Gf* is the measured diameter growth factor, Gf_{AS} is the growth factor of a fully soluble particle composed entirely of the same solute material, in this case ammonium sulphate ($\varepsilon_{\mathrm{AS}} = 1$), for the same humidified size and RH as for the observed particle. Gf_{AS} is often calculated from water activity data given by Tang and Munkelwitz (1994), which properly accounts for the non-ideal behaviour of the ammonium sulphate solution. The curvature of the wetted particle surface has to be considered by using the Kelvin factor to calculate the water activity a_{w} of the solution as given in eq. (1). The growth factor $Gf(a_{\mathrm{w}}, d_{\mathrm{d}}, \varepsilon)$, being a function of a_{w}, d_{d} and ε, (as discussed in Section 5) can then be translated into $Gf(\mathrm{RH}, d_{\mathrm{d}}, \varepsilon)$.

Frequent misconceptions are that this $\varepsilon_{\mathrm{AS}}$ can be interpreted as the real soluble volume fractions of the aerosol particles, or as if only ammonium sulphate were responsible for the water uptake. We strongly emphasize that this is not the case. The $\varepsilon_{\mathrm{AS}}$ should rather be interpreted as a model representation of a particle containing the same number of soluble ions or molecules (same Raoult's term in the Köhler equation, see Section 5.1.1), and accordingly having the same hygroscopic growth, as a particle of the same dry size with the volume fraction ε of the model salt.

We thus give boundaries for the ε-values for each group of hygroscopic growth, instead of *Gf*. The following values of ε could be used for most data sets to separate the hygroscopic groups (*Gf* values are for 100 nm dry size particles at RH = 90%):

nearly hydrophobic particles: $\varepsilon_{\mathrm{AS}} = 0.0$–$0.10$ ($Gf = 1.0$–1.11);
less-hygroscopic particles: $\varepsilon_{\mathrm{AS}} = 0.10$–$0.35$ ($Gf = 1.11$–1.33);
more-hygroscopic particles: $\varepsilon_{\mathrm{AS}} > 0.35$ ($Gf > 1.33$);
sea-salt particles (in marine air masses): $\varepsilon_{\mathrm{NaCl}} > 0.45$ ($Gf > 1.85$)

Ammonium sulphate (AS) or NaCl were used as reference salts to calculate soluble volume fractions ($\varepsilon_{\mathrm{AS}}$ and $\varepsilon_{\mathrm{NaCl}}$). Note that $Gf = 1.70$ for $\varepsilon_{\mathrm{AS}} = 1.0$ ($d_{\mathrm{d}} = 100$ nm, RH = 90%). Particles in the Aitken mode size range (20–80 nm dry diameter) tend to have somewhat lower values of ε_{AS} than particles in the accumulation mode size range (80–~500 nm dry diameter), so the values given above are only for guidance.

Most of the H-TDMA data was acquired at RH = 90%, but for some data sets, the reported RH in DMA2 was as low as 80%. To facilitate the intercomparison between the various observations, all *Gf* values were recalculated to RH = 90% using ammonium sulphate as model salt, as described by Swietlicki et al. (1999). While these corrected *Gf* values are rather insensitive to the choice of model salt, they may still be somewhat lower than the *Gf* values that would have been observed had the measurements actually been carried out at RH = 90%. This underestimation would occur if a significant volume fraction of the particle material goes into solution gradually between the actual DMA2 RH and RH = 90%.

Only a few field studies have performed scans in RH to explore the aerosol deliquescence and efflorescence behaviour and water uptake at low RH (McMurry and Stolzenburg, 1989; Zhang et al., 1993; Berg et al., 1998b; Dick et al., 2000; Santarpia et al., 2004; Sjogren et al., 2007a).

The figures with H-TDMA *Gf* data show the average *Gf* values for each data set, and are also those listed in the tables. The variability in *Gf* within each data set is not depicted in these figures.

3.3. Marine environments

Hygroscopic characteristics of particles in marine environments have been studied rather extensively in the past decade (Berg et al., 1998b; Swietlicki et al., 2000; Zhou et al., 2001; Vakeva et al., 2002a, b; Dusek et al., 2003; Massling et al., 2003; Massling et al., 2006; Tomlinson et al., 2007). These field studies

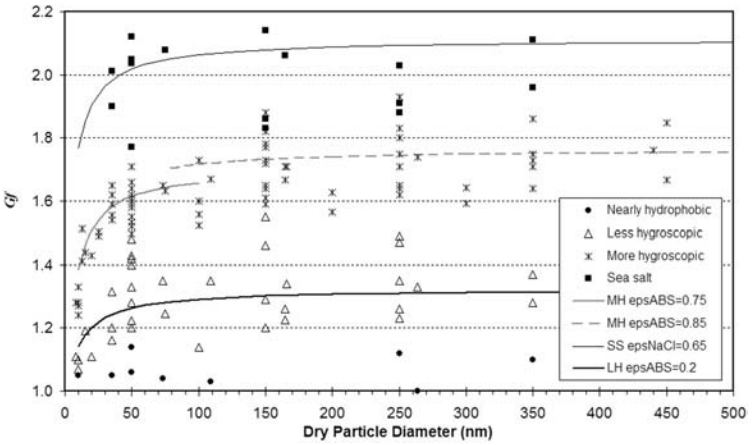

Fig. 5. Marine H-TDMA hygroscopic diameter growth factors *Gf* corrected to RH = 90%, when needed. 'epsABS' means that the soluble volume fraction was calculated using ammonium bisulphate as model reference salt; 'epsNaCl' is similar for NaCl. LH: less-hygroscopic group; MH: more-hygroscopic group; SS: sea salt group.

cover several of the major oceans (Atlantic Ocean, Pacific Ocean, Indian Ocean, Arctic Ocean), although each of them is often represented in the H-TDMA data set by one single cruise track (Fig. 4). In general, authors describe the appearance of one to four different hygroscopic particle groups, depending on air mass origin (Fig. 5, Table 1). A more-hygroscopic particle group is described as being ubiquitous. Growth factors of this particle group were observed to be larger than those found in urban or rural environments, and sometimes even larger than those for pure ammonium sulphate, implying that partly non-neutralized sulphate is a main component of this particle group. As an example, for 100 nm particle dry size at RH = 90%, $G_f = 1.70$ for pure ammonium sulphate ($\varepsilon_{\mathrm{AS}} = 1.0$), while $G_f = 1.79$ for pure ammonium bisulphate ($\varepsilon_{\mathrm{ABS}} = 1.0$). Oxidized sulphuric components deriving from emissions of dimethyl sulphide (DMS) from oceanic biota are typically only partly neutralized by ammonia in remote marine air masses. The more-hygroscopic particles are by far the most frequent, appearing in nearly 100% of all observations. During most of the time it is also the only hygroscopic particle group observed in remote marine environments in air masses with no land contact for the last five days.

Externally mixed sea salt particles with growth factors $G_f > 1.85$ ($\varepsilon_{\mathrm{NaCl}} > 0.45$) are often observed at high wind speeds in marine environments. Laboratory studies of the number size distribution of freshly generated sea salt particles (Martensson et al., 2003) show a peak in the sea salt particle number flux at around 100 nm in dry diameter, with significant contributions to the number fluxes extending down to 20 nm and probably beyond. Some H-TDMA studies in remote marine air masses have also reported such sea salt particles down to 35 nm in dry size (Berg et al., 1998b; Zhou et al., 2001). The source strength of sea salt particles is a very strong function of wind speed (see Martensson et al. (2003) and references therein) and is in general only important at wind speeds $>\sim 6$ m s^{-1}.

Although most of the wind-induced sea salt particle mass is found in the coarse fraction (>1 μm in diameter), by far the largest number concentrations are generated in the submicrometre size region. Considering that both the direct and indirect effects of aerosols on climate depend more strongly on the particle number concentration than on the mass concentration, the H-TDMA growth factor measurements in marine environments are highly relevant.

The calculated soluble volume fraction for particles in the sea-salt group is rather low, or $\varepsilon_{\mathrm{NaCl}} \approx 0.55$, when using pure NaCl as the reference salt. Applying the parametrization of water activity for filtered sea water samples (SW) by Tang et al. (1997) on the remote marine hygroscopic growth data yields soluble volume fractions significantly closer to unity, or $\varepsilon_{\mathrm{SW}} \approx 1.0$.

H-TDMA growth factors measured in the laboratory on samples of sea water taken in the Baltic Sea (1–2 m) and Atlantic deep water ($\sim$3000 m) show $G_f \approx 2.1$ for 100 nm dry size particles (Nilsson, 2007), in agreement with the EDB sea water (SW) water activity parametrization of Tang et al. (1997).

For the ubiquitous more-hygroscopic particle group, the corresponding soluble volume fraction is $\varepsilon_{\mathrm{ABS}} \approx 0.85$, and variable. The question arises what comprises the remaining particle volume in this the most frequently occurring remote marine aerosol particle group. The available chemical composition data (for instance (Ming and Russell, 2001; O'Dowd et al., 2004; Quinn and Bates, 2005; Kaku et al., 2006) indicate that organic compounds may make up a considerable mass fraction in some marine aerosol, in particular those influenced by marine biogenic activity.

Several studies noted that the appearance of externally mixed sea salt particles was far too limited in time to be entirely accountable to local wind speed fluctuations (Berg et al., 1998b; Swietlicki et al., 1999; Zhou et al., 2001). It has been suggested that this behaviour is caused by an uptake of sulphuric acid and subsequent release of hydrochloric acid, converting some of the sodium chloride to sodium sulphate, particles of which has a G_f of only 1.66 at 90% RH (Svenningsson et al., 2007). This formation of sodium sulphate salts will result in a significant drop in G_f to more resemble that of ammonium bisulphate. Observations of excess nonsea-salt sulphate on sea-salt particles (Andreae et al., 1986) support this idea. The short life time of

Table 1. Marine environments. Summary of H-TDMA measurements

Location	Dates	Dry size (nm)	*Gf* (90% RH) NH group	*Gf* (90% RH) LH group	*Gf* (90% RH) MH group	*Gf* (90% RH) Sea-salt group	DMA2 RH	Reference	Notes
Pacific Ocean (N-S transect)	Oct–Nov 1995	35		1.31	1.55	2.01	89%	Berg et al. (1998)	Ship-based
ACE-1		50		1.22	1.60	2.04			
		75		1.24	1.63	2.08			
		165		1.23	1.67	2.06			
Southern Ocean	Oct–Nov 1995	35			1.62		90%	Berg et al. (1998)	Ship-based
ACE-1		50			1.66	2.12			
		150			1.78	2.14			
Arctic Ocean	July–Aug 1996	15		1.19	1.44		90%	Zhou et al. (2001)	Ship-based
AOE-96		35		1.20	1.59	1.90			
16°–147°E and 70°–87.5°N		50		1.28	1.62	2.05			
		165		1.26	1.71	2.06			
NE Atlantic Ocean	June–July 1997	35	1.05		1.65		90%	Swietlicki et al. (2000)	Coastal
ACE-2		50	1.06	1.33	1.64				
Punta del Hidalgo, Tenerife (ES)		73	1.04	1.35	1.65				
16°19′W, 28°34′N, 63 m asl		109	1.03	1.35	1.67				
		166		1.34	1.71				
		264	1.00	1.33	1.74				
		440			1.76				
ACE-2	June–July 1997	10	1.05		1.28		90%	Swietlicki et al. (2000)	Free tropospheric
Izaña, Tenerife (ES)		10	1.05		1.24				
16°30′W, 28°18′N, 2367 m asl		50	1.14	1.40	1.61				
		50		1.43	1.62				
ACE-2	June–July 1997	35		1.16	1.54		90%	Swietlicki et al. (2000)	Coastal
Sagres-50 (P)		50		1.20	1.55				
8°57′W, 36°59′N, 50 m asl		100		1.14	1.60				
		150		1.20	1.65				
		250		1.23	1.65				
ACE-2	June–July 1997	50			1.64		75–80%	Swietlicki et al. (2000)	Ship-based
R/V Vodyanitsky		100			1.73				
29°–41°N and 8°–15°W		150			1.77				
NE Atlantic Ocean	Sept 1998	10		1.07	1.27		90%	Vakeva et al. (2002a, b)	Coastal
PARFORCE	June 1999	8		1.11	1.28				Ultrafine H-TDMA

Table 1. Cont'd.

Location	Dates	Dry size (nm)	*Gf* (90% RH) NH group group	*Gf* (90% RH) LH group	*Gf* (90% RH) MH group	*Gf* (90% RH) Sea-salt group	DMA2 RH	Reference	Notes
Mace Head (IRL)		10		1.10	1.33				During nucleation bursts
53°20′N, 9°54′W		20		1.11	1.43				
Atlantic Ocean (N-S transect)	Jan–Feb 1999	50		1.47	1.71		90%	Massling et al. (2003)	Ship-based
Aerosols-99		150		1.46	1.88				
		250		1.35	1.93				
Indian Ocean	Feb–Mar 1999	50		1.48	1.71		90%	Massling et al. (2003)	Ship-based
INDOEX		150		1.64	1.86				
		250		1.64	1.91				
Sea of Japan, East China Sea	Mar–Apr 2001	50			1.58		90%	Massling et al. (2006)	Ship-based
ACE-Asia		150			1.82				
Around southern Japan		250			1.83	2.03			
		350			1.86	2.11			
		50		1.42	1.61				
		150		1.46	1.72				
		250		1.47	1.71				
		350			1.64				
		50		1.20	1.52				
		150		1.29	1.61				
		250		1.26	1.65				
		350		1.28	1.71				
		50			1.59	1.77			
		150			1.59	1.83			
		250			1.62	1.88			
		350			1.73	1.96			
		50			1.62				
		150		1.55	1.73				
		250	1.12	1.49	1.75				
		350	1.10	1.37	1.75				
Southeastern Pacific Ocean	Nov 2003	13			1.51		85%	Tomlinson et al. (2007)	Ship-based
Stratus 2003		25			1.49				*RH*(DMA1) = 17%
		50			1.50				
		100			1.52				
		200			1.57				
		300			1.59				
		450			1.67				
		600			1.68				
							85%	Tomlinson et al. (2007)	Ship-based

Table 1. Cont'd.

Location	Dates	Dry size (nm)	*Gf* (90% RH) NH group group	*Gf* (90% RH) LH group	*Gf* (90% RH) MH group	*Gf* (90% RH) Sea-salt group	DMA2 RH	Reference	Notes
Stratus 2004	Dec 2004	13			1.41				*RH*(DMA1) = 27%
		25			1.50				
		50			1.53				
		100			1.56				
		200			1.63				
		300			1.64				
		450			1.85				
		600			1.93				

externally mixed sea salt particles with $G_f > 1.85$ indicates that this transformation is probably a rapid process in the remote marine atmosphere. Furthermore, model calculations, based on bulk chemical analysis of aerosol particles sampled over the Northeastern Pacific, overpredicted the hygroscopic growth by on average more than 30% (Kaku et al., 2006). The relative particle volume increase due to water uptake by a mixture of NH_4^+, Na^+, SO_4^{2-} and Cl^- ions at a given relative humidity is smaller if they are all internally mixed, compared to the case when ammonium sulphate and sodium chloride are externally mixed. The ZSR mixing rule (see Section 5.2) applied on these salts appears in this case not a good approximation for such processed sea salt aerosol particles (Cohen et al., 1987a; Kaku et al., 2006; Svenningsson et al., 2006a, b). These discrepancies in water uptake may be mitigated by proper ion pairing (Section 5.2.1).

To conclude, the present H-TDMA data sets are unable to reveal the exact chemical nature of the particles in the more-hygroscopic group. The three main alternatives are that these particles consist of either (i) partly neutralized DMS-derived sulphate particles or (ii) aged sea salt particles composed primarily of sea water inorganic compounds and sodium sulphate and (iii) aged sea salt particles composed of a mixture of sea water inorganic compounds and organic matter, or indeed combinations of these three compositions. All these chemical compositions could theoretically explain the observed hygroscopic growth with growth factors similar to that of pure ammonium sulphate or ammonium bisulphate salts (G_f = 1.70–1.79 for 100 nm particle dry size at RH = 90%). This is a reminder that the H-TDMA is unable to separate external mixtures with similar hygroscopic growth. It is likely that the composition of the particles in the more-hygroscopic group is dependent on the air mass history in a way not fully understood. Complementary measurements on individual particles are needed to determine the degree of external chemical mixture, for instance aerosol mass spectrometry, electron microscopy or combined volatility and hygroscopicity TDMA measurements.

Over warm and ice-free oceans, less-hygroscopic and nearly hydrophobic particles only appeared in air masses that were continentally influenced, although they were observed on the open ocean or at a coastal site. Continental contact in the last 24 hr is normally required for the nearly hydrophobic particles to be observed, after which they acquire enough soluble material by condensation to transform them into less- or more-hygroscopic particles. The frequency of occurrence of the less-hygroscopic particles is often between 0 and 60%, with higher values in air masses with more recent contact with continents.

The situation is strikingly different in the pack-ice covered summer Arctic Ocean. In this remote marine environment, nearly hydrophobic particles were quite frequently observed (Zhou et al., 2001). The Arctic oceanic biota are the likely source of these primary particles which, albeit weak in source strength, can readily be observed owing to the very low background aerosol concentrations (typically $<100\,cm^{-3}$) and the shallow Arctic marine boundary layer ($\sim$200 m) suppressing vertical dispersion. A similar source of biogenic primary aerosol particles have been suggested to be active also over warm oceans (Leck and Bigg, 2005), but there are as yet no H-TDMA observations that can firmly corroborate this hypothesis. The summer Arctic Ocean aerosol particles are nevertheless dominated by DMS-derived more-hygroscopic particles, even though atmospheric DMS and sulphate concentrations are very low in air masses that travelled for days or more over the pack-ice. Externally mixed sea salt particles were also observed over the pack-ice covered Arctic Ocean at high wind speeds ($>\sim$10 m s^{-1}), despite the fact the wind fetch over the open leads ($\sim$10% of the sea surface) between the ice floes is typically too small to generate considerable number fluxes of such particles via bubble-bursting processes (Nilsson et al., 2001).

3.4. Rural environments

H-TDMA measurements at rural continental background sites reported in the literature are almost entirely confined to

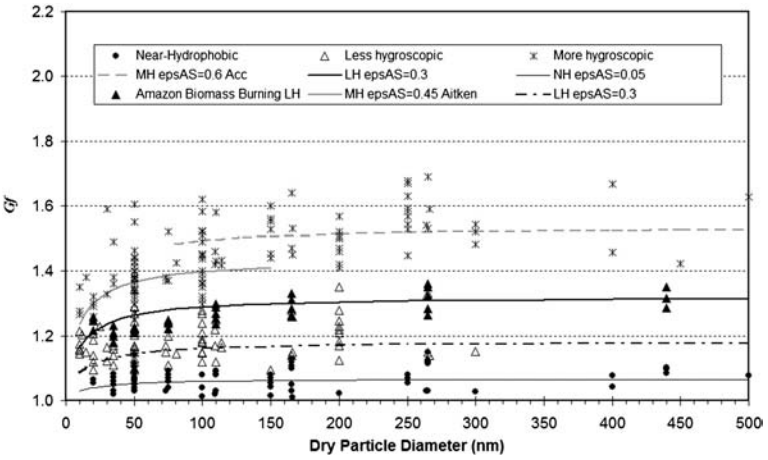

Fig. 6. Rural H-TDMA hygroscopic diameter growth factors *Gf* corrected to RH = 90%, when needed. 'epsAS' means that the soluble volume fraction was calculated using ammonium sulphate as model reference salt.

Europe and USA (Svenningsson et al., 1992; Pitchford and McMurry, 1994; Svenningsson et al., 1994; Svenningsson et al., 1997; Hameri et al., 2001b; Busch et al., 2002; Weingartner et al., 2002; Aklilu and Mozurkewich, 2004; Carrico et al., 2005; Ferron et al., 2005; Petaja et al., 2005; Van Dingenen et al., 2005; Gasparini et al., 2006; Ehn et al., 2007). The Amazon region in Brazil is the only other continental region where repeated non-urban measurements have been done (Zhou et al., 2002; Rissler et al., 2004, 2006) (Fig. 4). The lack of H-TDMA rural data from major continents such as Africa, Asia, Australia and Antarctica as well as large areas of North and South America is a serious drawback, as these areas represent a considerable fraction of the continental land mass. The anthropogenic emissions in developing countries are different in chemical and physical characteristics compared to those in USA and Europe, although not necessarily smaller in magnitude. In addition, natural sources have a dominating influence in many continental areas. The hygroscopic properties of these aerosols might therefore deviate from those observed in Europe and North America.

Rural sites exposed to aged air masses were originally expected to show an internally mixed aerosol, since atmospheric processes such as coagulation, condensation and in-cloud processing tend to gradually transform the aerosol towards a state of internal mixture. Closer to the multitude of sources typical of inhabited continental areas, external mixtures prevail, similar to those observed in urban areas. Since rural areas may experience both aged and freshly formed aerosols, the observations of the mixing state will vary accordingly.

Most of the H-TDMA measurements in rural environments shown in Fig. 6 were carried out during the last 15 yr. The classification of average *Gf* values into the various groups of hygroscopic growth was changed for some H-TDMA data sets in order to better comply with the classification given in Section 3.1.

Although the variability in *Gf* values appears to be large, a consistent picture emerges when applying this classification. For the particles in the accumulation mode size range ($> \sim$80 nm), the *Gf* fall into the three ranges characteristic for the near-hydrophobic (NH; $Gf = 1.0$–1.10), less-hygroscopic (LH; $Gf = 1.25$–1.35) and more-hygroscopic (MH; $Gf = 1.45$–1.60) particle groups.

The *Gf* values observed for the Amazonian biomass burning aerosol deviate from this pattern in the sense that they lack more-hygroscopic particles, and instead have intermediate *Gf* values between 1.15 and 1.3, still within the range of the less-hygroscopic particles. This is true for both relatively fresh (hours) and aged biomass burning smoke (Rissler et al., 2004, 2006). The reason is that the aerosol particles produced in open-air burning of biomass tend to contain a large fraction of organic components with limited water uptake capability since parts of the combustion is incomplete and takes place at fairly low temperatures (Mircea et al., 2005).

Figure 6 shows the average H-TDMA *Gf* values observed at rural sites (Table 2). Also shown are typical soluble volume fractions ε_{AS} (using ammonium sulphate as reference compound), although no fits to the data were made. Typical values of ε_{AS} are 0.05 for the nearly hydrophobic particle group (NH), 0.15 for the less-hygroscopic group (LH), and 0.6 for the more-hygroscopic group (MH). The Amazonian aerosol is best described using a $\varepsilon_{AS} = 0.30$ for the LH group [denoted moderately hygroscopic in Rissler et al. (2004, 2006)]. In addition, Amazonian aerosols show an external mixture with a group of nearly hydrophobic particles.

The Kelvin effect gives a lower diameter growth with decreasing diameter for the same chemical composition (constant ε). The more-hygroscopic Aitken mode particles ($< \sim$80 nm) have a tendency to show even smaller soluble volume fractions ($\varepsilon_{AS} \approx 0.45$) than the more-hygroscopic accumulation mode particles ($\varepsilon_{AS} \approx 0.60$). The spread in data is particularly large for the

Table 2. Rural environments. Summary of H-TDMA measurements

Location	Dates	Dry size (nm)	*Gf* (90% RH) NH group	*Gf* (90% RH) LH group	*Gf* (90% RH) MH group	DMA2 RH	Reference	Notes
San Pietro di Capofiume, Italy	Nov 1989	30		1.12	1.59	85%	Svenningsson et al. (1992)	Po Valley
44°39′N, 11°37′E, 11 m asl		50		1.13	1.61			
		100		1.15	1.58			
		150		1.10	1.55			
		200		1.12	1.57			
Grand Canyon, Arizona, USA	1990	50		1.15	1.38	89%	Pitchford et al. (1994)	
Navajo Generating Station Visibility		100		1.18	1.45			
35°16′N, 113°57′W		200		1.18	1.52			
		300		1.15	1.54			
		400	1.08		1.46			
Kleiner Feldberg, Germany	Oct–Nov 1990	50	1.14		1.43	85%	Svenningsson et al. (1994)	
50°12′N, 8°24′E, 825 m asl		150	1.06		1.44			
		300	1.03		1.48			
Great Dun Fell, UK	Apr–May 1993	50	1.06		1.34	90%	Svenningsson et al. (1997)	
EUROTRAC-GCE		75	1.06		1.37			
54°42′N, 2°30′W, 430 m asl		110	1.03		1.43			
		165	1.03		1.47			
		265	1.03		1.53			
Great Dun Fell, UK	Mar–May 1995	35		1.11	1.38	90%	Swietlicki et al. (1999)	Pennine ridge, England
EUROTRAC-2 PROCLOUD		50		1.12	1.44		Ground-based cloud experiment	
54°42′N, 2°30′W, 430 m asl		75		1.11	1.52			
		110		1.12	1.58			
		165		1.14	1.64			
		265		1.15	1.69			
Balbina, Brazil	Mar–Apr 1998	35	1.05	1.17	1.49	90%	Zhou et al. (2002)	Amazon rain forest
CLAIRE-98		50	1.05	1.16	1.38			125 km NE of Manaus, Brazil
−1°55.2′S, 59°28.1′W		73	1.03	1.17	1.38			Wet season, clean air
		109	1.02	1.22	1.42			
		166	1.01	1.26	1.45			
		264	1.03	1.32	1.54			
SE of Berlin, Germany	July–Aug 1998	50		1.12	1.43	90%	Busch et al. (2002)	80 km SE Berlin
LACE 98		100		1.12	1.49			
52°13′N, 14°7′E, 98 m asl		150	1.08		1.56			

Table 2 Cont'd

Location	Dates	Dry size (nm)	*Gf* (90% RH) NH group group	*Gf* (90% RH) LH group	*Gf* (90% RH) MH group	DMA2 RH	Reference	Notes
		250	1.08		1.63			
Hohenspeissenberg, Germany	Feb 1998	50	1.05		1.38	85%	Ferron et al. (2005)	
47°48′N, 11°1′E, 980 m asl		100	1.04		1.38			
		150	1.04		1.45			
		250	1.06		1.57			
	Aug–Sept 1998	50	1.12		1.34			
		100	1.08		1.44			
		150	1.07		1.53			
		250	1.07		1.59			
	Oct–Nov 1998	50	1.10		1.36			
		100	1.01		1.52			
		150	1.01		1.60			
		250	1.06		1.68			
Hyytiälä, Finland	Apr 1999	10		1.16	1.35	90%	Hameri et al. (2001a, b)	Boreal forest
BIOFOR III		15		1.15	1.38			
61°51′N, 24°17′E, 181 m asl		20	1.12	1.32				
		35		1.16	1.36			
		50		1.15	1.32			
		73		1.15	1.37			
		109		1.17	1.46			
		166		1.15	1.53			
		266		1.14	1.59			
Monte Cimone Observatory (Italy)	June–July 2000	50		1.22	1.37	90%	Van Dingenen et al. (2005)	Northern Europe
MINATROC		100		1.21	1.39			
44°11′N, 10°42′E, 2165 m asl		200		1.21	1.47			
		50		0.89	1.27			NW Europe
		100		1.18	1.30			
		200		0.94	1.47			
		50		1.10	1.25			Western Europe
		100		1.24	1.32			
		200		1.22	1.46			
		50		1.29	1.31			Eastern Europe
		100		1.28	1.40			
		200		1.28	1.41			
		50		1.27	1.33			Mediterranean
		100		1.24	1.36			
		200		1.35	1.50			
		50		1.16	1.30			Africa, no dust
		100		1.27	1.31			
		200		1.23	1.42			
		50		1.29	1.40			Saharan dust event
		100		1.15	1.35			
		200		1.17	1.46			
Jungfraujoch, Switzerland	March 2000	50			1.55	90%	Weingartner et al. (2002)	Mountain site

Table 2. Cont'd.

Location	Dates	Dry size (nm)	*Gf* (90% RH) NH group	*Gf* (90% RH) LH group	*Gf* (90% RH) MH group	DMA2 RH	Reference	Notes
46.33°N, 7.59°E, 3580 m asl		100		1.62				Examples of data
		250			1.67			
Balbina, Brazil	July 2001	35	1.02	1.14		90%	Rissler et al. (2004)	Clean period
CLAIRE-2001		50	1.07	1.17				Amazon rain forest 125 km NE of Manaus, Brazil
		110	1.08	1.25				
		165	1.05	1.28				
		265	1.15	1.33				
		35	1.03	1.18				Recent Biomass burning
		50	1.04	1.21				
		75	1.07	1.25				
		110	1.09	1.30				
		165	1.12	1.33				
		265	1.12	1.36				
		35	1.02	1.21				Aged Biomass burning
		50	1.03	1.21				
		75	1.04	1.24				
		110	1.08	1.29				
		165	1.13	1.31				
		265	1.15	1.35				
Golden Ears, USA	Aug 2001	81		1.14	1.43	80%	Aklilu and Mozurkewich (2004)	
Pacific 2002 49°12′53″N, 122°34′55″W, 203 m asl		114		1.16	1.43			
Eagle Ridge, USA	Aug 2001	50		1.17	1.40	80%	Aklilu and Mozurkewich (2004)	
Pacific 2002		81		1.14				
49°3′8″N, 122°14′45″W, 300 m asl		114		1.18	1.42			
Yosemite Valley, California, USA	July–Sept 2002	100		1.19	1.45	90%	Carrico et al. (2005)	
YACS 37°42′N, 119°42′W, 1615 m asl		200		1.21	1.51			
Near Ouro Preto, Rondonia, Brazil	Sept–Nov 2002	20	1.07	1.25		90%	Rissler et al. (2006)	Fazenda Nossa Senhora Aparecida

Table 2. Cont'd.

Location	Dates	Dry size (nm)	*Gf* (90% RH) NH group	*Gf* (90% RH) LH group	*Gf* (90% RH) MH group	DMA2 RH	Reference	Notes
LBA-SMOCC		35	1.06	1.20				Dry period
10° 45′44″S, 62°21′27″W, 315 m asl		50	1.07	1.23				Biomass burning
		75	1.07	1.22				
		110	1.08	1.24				
		165	1.10	1.26				
		265	1.12	1.26				
		440	1.10	1.29				
		20	1.07	1.26				Transition period
		35	1.07	1.23				Biomass burning
		50	1.07	1.22				
		75	1.08	1.24				
		110	1.09	1.26				
		165	1.10	1.26				
		265	1.12	1.28				
		440	1.10	1.32				
		20	1.06	1.22				Wet period
		35	1.08	1.21				
		50	1.09	1.21				
		75	1.09	1.24				
		110	1.09	1.27				
		165	1.11	1.29				
		265	1.13	1.32				
		440	1.09	1.35				
Hyytiälä, Finland	Mar–Apr 2003	10		1.14		89%	Petaja et al. (2005)	Before nucleation
QUEST		20		1.09				Clean Artic air masses
61°51′N, 24°17′E, 181 m asl		50		1.10				
		10		1.15				Arctic and Estonia
		20		1.21				
		50		1.24				
		10		1.22				Arctic Kola
		20		1.25				
		50			1.46			
		10		1.17				Right after nucleation occurring
		20		1.19				Clean Arctic
		50		1.22				
		10		1.27				Arctic and Estonia
		20		1.29				
		50		1.34				
		10		1.28				Arctic Kola
		20		1.26				
		50			1.44			
ARM SGP, Oklahoma, USA	May 2003	12		1.20		85%	Gasparini et al. (2006)	
36°37′N, 97°30′W, 315 m asl		25		1.23				

Table 2. Cont'd.

Location	Dates	Dry size (nm)	*Gf* (90% RH) NH group	*Gf* (90% RH) LH group	*Gf* (90% RH) MH group	DMA2 RH	Reference	Notes
		50		1.29				
		100			1.40			
		200			1.51			
		300			1.52			
		450			1.42			
		600			1.35			
Hyytiälä, Finland	Apr–May 2005	20		1.14		88%	Ehn et al. (2007)	Boreal forest, night
QUEST		30		1.16				
61°51′N, 24°17′E, 181 m asl		50		1.20				
		20		1.30				Boreal forest, midday
		30		1.33				
		50		1.34				

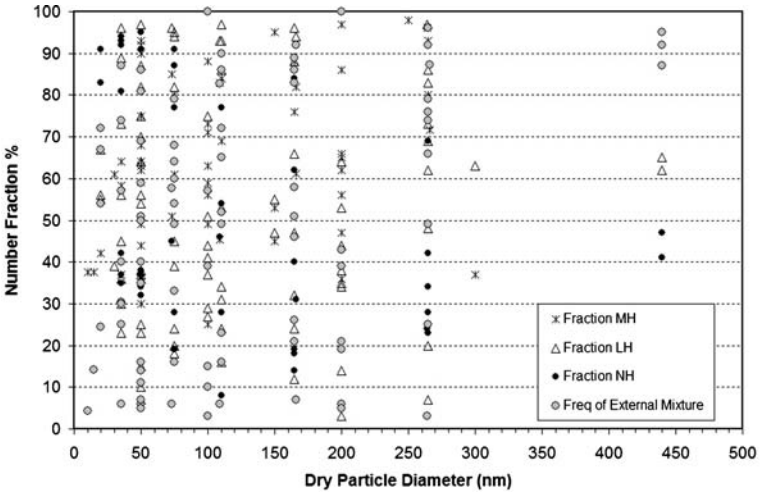

Fig. 7. The frequencies of external mixtures in rural environments—as observed by the H-TDMA and reported—and the number fractions of each hygroscopic group.

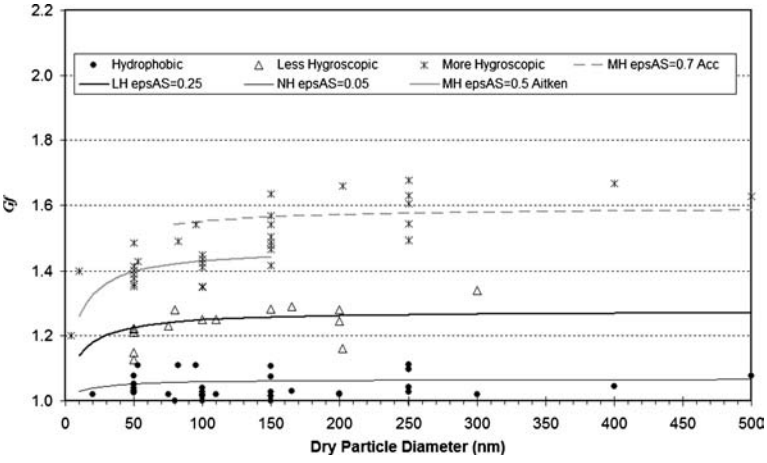

Fig. 8. Urban H-TDMA growth factors *Gf* corrected to RH = 90%, when needed.

Aitken mode particles. This is most likely due to larger variability in the chemical composition as Aitken mode particles more reflect the chemical characteristics of the multiple sources. As growth by condensation and coagulation are the most important transformation processes for this size range, *Gf* depend strongly on the properties of the condensing gases. Most of the measurements showing low *Gf* for the smallest more-hygroscopic particles come from studies in various forest dominated areas in Europe and USA.

The differences in chemical composition and solubility (ε_{AS}) between the Aitken and accumulation mode particles are most probably due to in-cloud processing. Some of the Aitken mode particles may be activated to form cloud droplets, most of which will escape precipitation scavenging and evaporate in the cloud outflow region. If water-soluble material was added to the cloud droplet by oxidation of dissolved gases such as SO_2, the returned particles will be both slightly larger and more soluble than the particle on which the droplet formed.

Figure 7 shows the frequencies at which external mixtures were observed at rural sites, and the number fractions of the less- and more-hygroscopic particle groups. Again, these values are averages for each rural H-TDMA data set, if and when reported. It is clear that the frequencies of external mixtures vary very strongly between data sets, which is also observed to be the case at many individual sites. There is a tendency that external mixtures are more often observed at larger particle sizes than for the Aitken mode particles. Except in Amazonia, more-hygroscopic particles are present in nearly all rural H-TDMA studies. The less-hygroscopic particle group dominates at sites with a large mass fraction of organic compounds, such as during particle formation events in the boreal forest (Hyytiälä, Finland) and in Amazonia. The nearly hydrophobic group is present only in areas which are strongly influenced by combustion, such as the Po Valley, central Germany and the Amazon.

During recent years, the boreal regions have gained attention as an important source of particles in areas lacking anthropogenic emissions. For the Scandinavian region, Tunved et al. (2006a, b) have shown both qualitatively and quantitatively that the monoterpene emissions from the boreal forest at high latitudes in Europe potentially contribute to particle generation with an apparent mass yield in the range of approximately 5–10%. These emissions seem to rapidly establish a particle population with concentrations of some 1000 cm^{-3} in a size range between 30 and 100 nm. Monoterpene oxidation products have further been identified in freshly formed particles (O'Dowd et al., 2002; Cavalli et al., 2006), and several investigations of new particle formation events during the biologically active seasons indicate that biogenic aerosol precursor gases are necessary to support the observed mass increase during particle formation events. The process is most efficient during the extended summer period, April–September, when both emissions of monoterpenes and new particle formation events are most commonly observed. Chamber studies show that the hygroscopic growth of particles generated in a mixture of monoterpenes and oxidants, mainly ozone, yield growth factors in the range $Gf = 1.07–1.12$ (Virkkula et al., 1999; Saathoff et al., 2003). In the field, studies performed at the boreal site Hyytiälä (Hameri et al., 2001b) showed a larger fraction of less-hygroscopic particles during new particle formation events, indicating the role of condensing organics. The nucleation mode was found to be internally mixed with a growth factor $Gf = 1.1–1.15$ (at 90% RH). Concerning the CCN capability of the organic aerosols, findings by Hartz et al. (2005) show that biogenic SOA derived from selected monoterpenes act as excellent CCN, with an average activation diameter around 50 nm at 1% supersaturation. A study by Kerminen et al. (2005) further present a direct link between new particle formation events and subsequent activation of the freshly formed particles into cloud droplets at a remote site in boreal region of Northern Finland. Since the emissions believed to contribute to the aerosol above the boreal forest is temperature dependent, increasing temperatures are likely accompanied by increasing emissions and thus also increased amount of CCN. This means that forest emissions and subsequent formation of particles constitute an interesting feedback that deserves further investigation.

3.5. Urban environments

Urban areas are significant sources of anthropogenic aerosol particles, and the investigation of their physico-chemical properties is therefore of special interest. The hygroscopic properties of submicrometre urban aerosol particles have strong impact on climate, but also on visibility in heavily polluted areas. The health effects on humans exposed to airborne particles in densely populated conurbations depend on the dose and site of deposition of the particles in the human airways, which in turn depend on the actual size that the particles attain in the humid respiratory tract (Londahl et al., 2007). Despite these obvious research needs, hygroscopic growth measurements in urban environments are rather scarce up to now (McMurry and Stolzenburg, 1989; McMurry et al., 1996; Cocker et al., 2001; Baltensperger et al., 2002a; Chen et al., 2003; Massling et al., 2005). Most of these measurements were limited to at most several weeks at urban background stations, and very few measurements close to traffic sources like in street canyons have been published, such as in Milan (Baltensperger et al., 2002a).

Overall, the various urban H-TDMA studies found a persistent separation of the hygroscopic submicrometre growth distributions into at least two, or sometimes three groups than can be classified as being nearly hydrophobic, less-hygroscopic and more-hygroscopic particles (Fig. 8, Table 3).

Particles in the nearly hydrophobic group can be assumed to largely consist of freshly emitted combustion particles containing high mass fractions of soot and water-insoluble organic compounds. The less-hygroscopic particles may, in many cases,

Table 3. Urban environments. Summary of H-TDMA measurements

Location	Dates	Dry size (nm)	*Gf* (90% RH) NH group	*Gf* (90% RH) LH group	*Gf* (90% RH) MH group	DMA2 RH	Reference	Notes
Claremont, California, USA	Summer 1987	50	1.03	1.15		89%	Zhang et al. (1993)	
SCAQS		200	1.02	1.25				
34°1′N, 117°42′E		400	1.04		1.67			
		500	1.08		1.63			
Neuherberg, Germany	Jan–Feb 1997	50	1.05		1.36	90%	Tschiersch et al. (1997)	North of Munich
48°9′N, 11°20′E		75	1.02	1.23				
		110	1.02	1.25				
		165	1.03	1.29				
		300	1.02	1.34				
Milano (IT)	June–July 1998	20	1.02			90%	Baltensperger et al. (2002)	Bresso & Verzago, Milano
PIPAPO		50	1.03	1.21				
45°32′N, 9°12′E, 130 m asl		100	1.02	1.25				
		200	1.02	1.28				
Bavaria, Germany	Feb–Mar 1998	50	0.99		1.49	85%	Ferron et al. (2005)	
48°8′N, 11°35′E		100	1.00		1.42			
		150	1.01		1.47			
		250	1.10		1.60			
	Sept 1998	50	1.04		1.38			
		100	1.03		1.35			
		150	1.01		1.42			
		250	1.10		1.49			
	Nov 1998	50	1.03		1.40			
		100	1.01		1.45			
		150	1.01		1.54			
		250	1.03		1.63			
Bavaria, Germany, cont.	Mar 1998	50	1.03		1.38			
48°8′N, 11°35′E		100	1.01		1.42			
		150	1.03		1.50			
		250	1.11		1.68			
	Aug 1998	50	1.08		1.35			
		100	1.04		1.44			
		150	1.03		1.54			
		250	1.04		1.63			
	Oct 1998	50	1.05		1.41			
		100	1.03		1.41			
		150	1.03		1.48			
		250	1.03		1.54			
Pasadena, California (USA)	Aug–Sept 1999	50	1.05	1.13		89%	Cocker et al. (2001)	
39°9′N, 118°8′W		50		1.22				
		150	1.11		1.64			
Leipzig, Germany	May–Aug 2000	50	1.05	1.22	1.39	92%	Massling et al. (2005)	8 months

Table 3. Cont'd.

Location	Dates	Dry size (nm)	*Gf* (90% RH) NH group	*Gf* (90% RH) LH group	*Gf* (90% RH) MH group	DMA2 RH	Reference	Notes
51°20′N, 12°20′E	and Nov 2000–Feb 2001	150	1.08	1.28	1.57			
Tokyo, Japan	Nov 2000	80	1.00	1.28		83%	Mochida et al. (2006)	
35°41′N, 139°44′E		100	1.00		1.35			
		150	1.00		1.49			
Taipei, Taiwan	Oct–Dec 2001	53	1.11		1.43	90%	Chen et al. (2003)	
25°2′N, 121°38′E		82	1.11		1.49			
		95	1.11		1.54			
		202		1.16	1.66			
Atlanta, Georgia, USA	Aug 2002	4			1.20	90%	Sakurai et al. (2005)	In plume from point
ANARChE 33°46′N, 84°25′W		10			1.40			source (high SO_2) during nucleation

be moderately transformed combustion particles containing soot, partly oxygenated organic compounds and condensed inorganic matter.

There are surprisingly few H-TDMA studies on freshly emitted traffic exhaust particles, and the two that are available are for diesel aerosols (Weingartner et al., 1997; Grose et al., 2006). Weingartner et al. (1997) found that the highly agglomerated diesel soot particles were nearly hydrophobic. As an example, growth factors at RH = 90% are $G_f \approx 1.01$–1.02 for particles in the (dry) size interval 50–110 nm. In the same study, Weingartner et al. (1997) show that carbon soot particles, generated by spark discharge between two graphite electrodes, even decreased in (mobility) size following humidification, due to restructuring of the highly agglomerated soot particles. Diesel particles were found to undergo less restructuring, and also contained small mass fractions of hygroscopic material such as sulphates and water-soluble organic compounds causing them to grow slightly when humidified. In urban H-TDMA field studies, these fresh diesel soot particles would definitely be categorized as being nearly hydrophobic.

Grose et al. (2006) used a nano-TDMA setup to study the volatility and hygroscopicity of 4–15 nm diesel exhaust particles downstream of a CRT (Continuously Regenerating Trap) diesel particle filter, and could confirm that these particles consisted primarily of sulphates.

In the urban H-TDMA studies, the number fraction of the nearly hydrophobic and less-hygroscopic particle groups often decrease with size, in accordance with that of the soot number size distribution from traffic emissions that peak at about 50–100 nm.

It is likely that freshly emitted nearly hydrophobic particles age in the atmosphere and transform, by condensation of vapours and to a lesser extent by coagulation, into less-hygroscopic aerosol particles. However, the time scales for these processes taking place either in the urban air shed or in the urban plume downstream of the city are currently not well understood and should be subject to further studies. More detailed investigations of freshly emitted traffic related particles, for example in a street canyon, are also strongly recommended in order to increase our understanding regarding particle transformation processes on short time scales.

The more-hygroscopic urban aerosol particles showed growth factors that are quite similar to those found in rural environments. The more-hygroscopic particle fraction can in most cases be attributed entirely to the regional background aerosol entering the urban air shed. The external mixture observed by the H-TDMA can then be used as an estimate of the importance of the regional background as opposed to the local urban sources that provide the nearly hydrophobic particles. The situation is more complex for the less-hygroscopic particle group, for which both regional and local sources are likely contributors.

The attribution of more-hygroscopic particles to the regional background aerosol may not be correct in urban environments affected by biomass combustion and wood burning aerosols. Efficient combustion of biofuels generate an aerosol that is rich in alkali salts but contains very little organic compounds and soot. These biomass combustion aerosol particles can thus be very hygroscopic, with growth factors very similar to those of the more-hygroscopic group (Rissler et al., 2005). This is in sharp contrast to the hygroscopic properties of particles

emitted from low-temperature incomplete combustion of biofuels, as discussed already for Amazonian biomass burning aerosols.

Using ammonium sulphate as reference salt, the soluble volume fractions of the more-hygroscopic group are grouped around $\varepsilon_{AS} \approx 0.7$ for the accumulation mode size range, and $\varepsilon_{AS} \approx 0.5$ for the Aitken mode size range. This in an indication that the more-hygroscopic particles may have been processed during transport in the regional background air, resulting in a higher soluble fraction for the larger particles.

3.6. *Free tropospheric*

Ground-based aerosol measurements at sites that can be claimed to be representative of conditions in the free troposphere (FT) are scarce. H-TDMA data from FT sites are even more rare, and we are only aware of three such sites. These are from the high alpine research station Jungfraujoch in the Bernese Alps in Switzerland (3580 m a.s.l.) (Weingartner et al., 2002; Sjogren et al., 2007a), the Izaña baseline observatory station on the Canarian island of Tenerife in the northeastern Atlantic (2367 m a.s.l.) (Swietlicki et al., 2000), and finally the Monte Cimone observatory in northern Italy (2165 m a.s.l.) (Van Dingenen et al., 2005). Although these sites are located in the lower free troposphere, they are also influenced by injections of more polluted planetary boundary layer (PBL) air by thermal convection during afternoons.

At Jungfraujoch, extensive field campaigns were conducted during summer and winter in the years 2000, 2002, 2004 and 2005 when also the particle hygroscopic properties were measured (Weingartner et al., 2002; Sjogren et al., 2007a). Non-disturbed lower free tropospheric conditions were only guaranteed in the winter. A low-temperature H-TDMA system (Weingartner et al., 2002) was therefore employed to avoid volatilization of semi-volatile material. These measurements were performed close to ambient temperature (i.e. $T = -10^{\circ}$C during winter). Such measurements at subzero temperatures are thus representative of ambient conditions, as the aerosol was not exposed to room temperature at any time before and during analysis. Wintertime FT average growth factors at RH = 85% are $G_f = 1.33$–1.50 for particles in the (dry) size interval 50–250 nm, corresponding to ε_{AS} between 0.53 and 0.92 (Weingartner et al., 2002; Sjogren et al., 2007a). These hygroscopic growth factors were shown to be well predicted from measured chemical composition using the ZSR mixing rule (Section 5.2) when taking into account both organic and inorganic species. Lower hygroscopic growth factors encountered during the PBL influenced summer conditions were caused by a significantly higher fraction of organic compounds in the fine aerosol (typically 68% in summer compared to 42% in winter). When scanning DMA2 RH in the range 10–85%, no signs of deliquescence or efflorescence behaviour were seen (Fig. 9). Such continuous growth is expected and has been reported for complex mixtures with an increasing number of organic components [e.g. (Marcolli and Krieger, 2006)]. At Jungfraujoch, the FT aerosol in general showed a higher degree of external mixing than the PBL influenced aerosol.

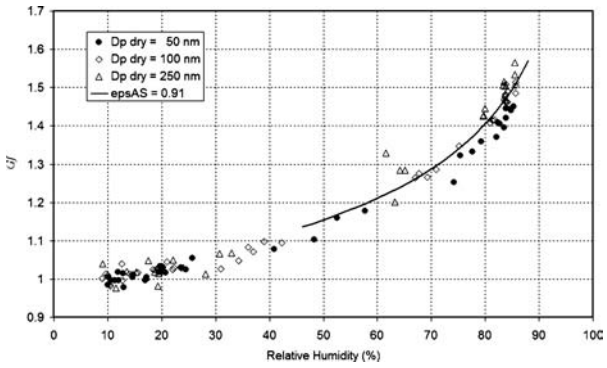

Fig. 9. A typical humidogram of free tropospheric aerosol particles with dry diameters = 50, 100 and 250 nm measured during in winter 2000 at Jungfraujoch. The individual data points were acquired with a temporal resolution of 5 min. The absence of distinct phase changes suggests that the aerosol at JFJ is present as solution droplets in a broad RH range. The solid line shows the calculated hygroscopic behaviour for particles with $\varepsilon_{AS} = 0.91$ at $T = -10\ ^{\circ}$C.

The Monte Cimone site not far south of Jungfraujoch is typically located in a transition layer between the planetary boundary layer and the free troposphere, and H-TDMA data in FT air is only available for a short 8 h time period during an episode with subsiding air arriving from the northeast (Van Dingenen et al., 2005). Monte Cimone FT growth factors at RH = 90% are $G_f \approx 1.21$ for the less-hygroscopic particle group and $G_f = 1.37$–1.47 for the more-hygroscopic particles in the (dry) size interval 50–200 nm, corresponding to ε_{AS} between 0.45 and 0.62 (Van Dingenen et al., 2005). An external mixture was seen in roughly half of the scans at 100 and 200 nm dry size. As for the Jungfraujoch site, water-soluble organic matter was required to account for the observed growth factors.

Despite efforts to separate time periods with FT air unperturbed by recent influence from the marine boundary layer, only limited conclusions could be drawn from the H-TDMA measurements performed at the Izaña observatory on the island of Tenerife (Swietlicki et al., 2000). The H-TDMA instrument used was furthermore designed for studies of nucleation mode particles, and only measured the hygroscopic growth at dry sizes of 10 and 50 nm. While the 10 nm FT particles were nearly hydrophobic, the 50 nm particles in FT air were predominately less-hygroscopic with $G_f \approx 1.4$ at RH = 90% (number fraction ~75%).

Considering the importance of the FT aerosol as an efficient long-range transport pathway and the climatic effect of mid-tropospheric clouds formed on this aerosol, it is surprising that H-TDMA data from the free troposphere are so few. H-TDMA instruments operated from aircraft as well as long-term

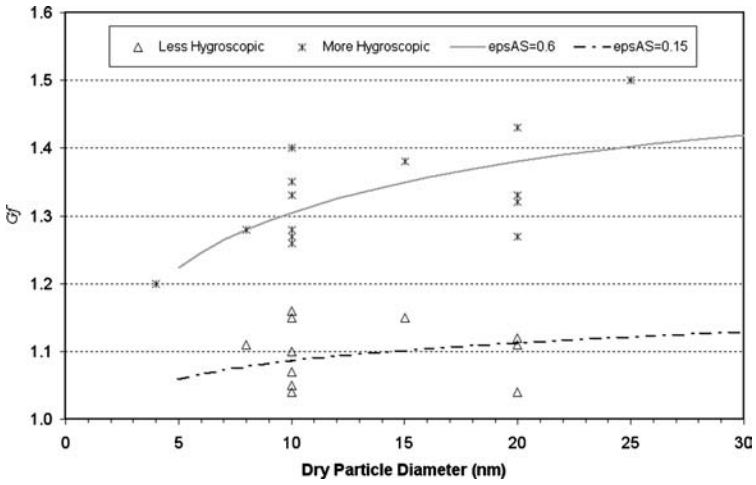

Fig. 10. Nucleation event H-TDMA growth factors *Gf* corrected to RH = 90%, when needed. Only *Gf* data acquired during clear new particle formation events are included.

H-TDMA measurements at mountain sites exposed to a variety of air masses would improve this situation considerably.

3.7. Nucleation, various environments

Several H-TDMA studies have focused on nucleation mode particles (dry diameters $< \sim 30$ nm), conducted in a variety of environments. The nucleation mode particles can be classified into those formed in the atmosphere during nucleation events and those emitted into the atmosphere from human activities, such as vehicle emissions. These two types of aerosols are not always easily separated. However, most of the studies focusing on the hygroscopic properties of nucleation mode particles were aiming at determining particles formed during nucleation events.

The hygroscopic properties of nucleation mode particles provide constraints on particle composition. While these data may help to formulate hypotheses on composition and to exclude unlikely composition alternatives, they cannot however provide unambiguous information on composition.

Nucleation event H-TDMA data are available in urban and urban background area of Helsinki, Finland (Vakeva et al., 2000), Atlanta, USA (Sakurai et al., 2005), and Marseille, France and Athens, Greece (Petaja et al., 2007), in boreal forest in Hyytiälä, Finland, (Hameri et al., 2001b), in coastal environments at Mace Head, Ireland (Vakeva et al., 2002a) and at the Gosan site, located on Jeju Island near the Korean peninsula (Buzorius et al., 2004). The *Gf* data acquired during clear new particle formation events are shown in Fig. 10.

Several of the observed atmospheric nucleation events take place over wider regions simultaneously, and the formation of particles is often followed by their growth to Aitken mode sizes (Kulmala et al., 2004). These regional nucleation events have been characterized in clean background air masses over a boreal forest (Hameri et al., 2001b), in an urban environment of Atlanta (Sakurai et al., 2005), in a Mediterranean environment (Petaja et al., 2007) and on Jeju Island (Buzorius et al., 2004).

During nucleation events at the boreal forest site in Finland the G_f -distribution was usually mono-modal, showing strong diurnal variation for both 10 and 20 nm particles with minimum G_f values during nighttime and maximum G_f during midday periods. A similar diurnal variation was observed also for the rural background particles during days with no nucleation events. In the boreal environment, the G_f varied between 1.08 and 1.28 for 10 nm particles and between 1.08 and 1.33 for 20 nm particles. Similar G_f values and diurnal cycle were also observed at a background site in Helsinki during one regional nucleation event (Vakeva et al., 2000). During nucleation events on Jeju island south of the Korean peninsula the G_f for 25 nm particles was as high as 1.5 (at 83% RH).

According to a case study by Petaja et al. (2005), the growth factors of nucleation mode particles at the same boreal forest site were slightly influenced by the air mass history, with higher growth factors in an aged polluted air mass. This G_f air mass dependence was, however, much stronger for the Aitken mode particles than for the nucleation mode particles, since the larger particles were exposed to the polluted environment for a longer time. Extended datasets, however, are needed to verify this.

Coastal nucleation events related to aerosol formation from exposed tidal zone sea-bottom were measured at Mace Head in Western Ireland (Vakeva et al., 2002a). The observed nucleation events were classified into several different types based on the origin of the air masses. Nucleation in clean marine air masses had $G_f = 1.1$ for both 8 and 10 nm particles. During nucleation events where the air masses had passed over two or several tidal regions, 8 nm (and also 10 nm) growth factors on the average seemed to have a diurnal behaviour. If particles were observed in the morning or nighttime when H_2SO_4 production and concentration were low, the growth factors were also low ($G_f = 1.05$ or less), but during midday and early afternoon higher growth factors were observed. This behaviour was similar to that described above for the boreal forest site (Hameri et al., 2001b).

The growth factor values were extremely variable during days when particle formation took place in air masses arriving over the continent. Low growth factors were observed sometimes during the strongest particle production times but, on the other hand, very high growth factors were also seen ($G_f = 1.3$ for 8 nm particles). During these days the precursor gases, and also water-soluble condensable gases, were probably abundant. In particular, high sulphuric acid concentrations were observed coinciding with the high growth factors. A positive correlation between nucleation mode G_f and measured sulphuric acid concentrations was seen also in a boreal forest environment (Ehn et al., 2007). The nucleation mode particles are likely to be more sensitive to variations in the concentrations of condensable gas-phase compounds than the larger Aitken and accumulation mode particles.

The hygroscopic properties of urban background nucleation mode particles were measured in Helsinki, Finland (Vakeva et al., 2002b) and in Atlanta (Sakurai et al., 2005). In Helsinki, the G_f—distribution for 10 nm particles was mostly bi-modal during the winter time measurement period, with mean $G_f = 1.04$ and 1.26. For 20 nm particles, the observed growth factors were $G_f = 1.04$ and 1.27. In spring time, the background nucleation mode aerosol was mainly mono-modal with a mean $G_f = 1.15$ for 10 nm particles.

In Atlanta, the growth factors were much higher, $G_f = 1.4$ for 10 nm particles for both regional nucleation event and pollution plume particles, most likely due to the high concentrations of SO_2 and thus also sulphuric acid. In plumes from point sources containing elevated levels of SO_2 and other gases, a $G_f \approx 1.2$ for 4 nm particles was measured indicating soluble volume fractions similar to that of the 10 nm particles. During periods of no nucleation, a bi-modal G_f distribution was observed for 10 nm particles with $G_f = 1.3$–1.4 and 1.0–1.1.

The water solubility of the condensing species can be determined by following the evolution of hygroscopic properties of the growing nucleation mode particles (Kulmala et al., 2001). In a boreal environment Kulmala et al. (2001) estimated that the ratio between the condensation fluxes of water soluble to insoluble material was between 0.7 and 1.4, that is, the fluxes were of similar magnitude. In the urban background of Athens, Greece, Petaja et al. (2007) found that water soluble compounds dominated the growth of newly formed particles during nucleation events in air masses that were affected by urban pollution, whereas condensation of insoluble compounds were more pronounced during clean periods.

It is evident that H-TDMA measurements can provide important pieces of information regarding the detailed chemical and physical processes leading to new particle formation and the compounds that participate in the subsequent growth to larger sizes. The hygroscopic properties affect the size distribution of the nucleation mode particles at the prevailing ambient humidities, and thus also coagulation and deposition rates as well as their growth by condensation. These properties therefore potentially influence the probability of the newly formed particles to reach sizes where they may perturb the radiative balance by direct light scattering or by contributing to the CCN population.

3.8. Recommendations for future H-TDMA studies

For all types of atmospheric aerosol studies involving H-TDMA measurements, it is evident that there is still a great demand for continuous long-term H-TDMA data sets. Although the data reviewed here show rather high degrees of consistency for a given type of air mass, there is still not enough information available to fully account for the observed *Gf* variability.

The geographical coverage is also poor, as can be seen in Fig. 4. There is a need for additional H-TDMA data in regions of the globe where human activities have a significant influence on the magnitude of the direct and indirect aerosol forcing of climate. The vertical coverage is even poorer, with very limited data from the free troposphere.

3.8.1. Complementary data. The various H-TDMA studies described above have not been performed in splendid isolation, but rather as one important set of observations complementing other parallel measurements regarding the various chemical and physical properties of the same aerosol and the air mass in which it travels. The set of complementary observations required for an adequate interpretation of the H-TDMA data depends on the purpose of the atmospheric study in question, whether being a characterization study, a closure experiment, or a process study, or combinations thereof.

H-TDMA instruments produce relative data in the sense that they give information regarding the number fraction of aerosol particles of a certain dry size that displays a certain hygroscopic growth. In order to convert this relative information into absolute terms (number concentrations of particles with a certain hygroscopic behaviour), the H-TDMA data sets need to be accompanied by parallel measurements of the dry number size distribution, using DMPS or SMPS instruments. This information is indispensable for all closure studies involving H-TDMA data (Section 5.4), and essential also for most characterization and process studies.

So called hygroscopicity closure studies also require size-resolved information regarding the aerosol particle chemical composition, most importantly the water-soluble mass fraction, and is discussed further in Section 5.4.1. Analysis of the inorganic mass fraction is essential since it typically accounts for most of the hygroscopic growth.

3.8.2. Presentation of H-TDMA data. Recommendations for the operation of H-TDMA instrument during field experiments can be found in Sections 2.1 and 2.3 above, including which auxiliary parameters that should be accompanying each H-TDMA data set.

One aim of H-TDMA studies on atmospheric aerosols is to provide data that can be used to develop and validate models on various spatial scales that include a size-resolved and number-based description of the aerosol, as is the case for several

state-of-the-art Chemical Transport Models (CTM) and General Circulation Models (GCM). This should be kept in mind when presenting H-TDMA data.

While this can often be achieved using tables, it would be beneficial to aid future data users by providing parametrizations (see Section 4 below) of $Gf(\mathrm{RH},d_\mathrm{d})$—or $\varepsilon(d_\mathrm{d})$—accompanied with a clear statement for which conditions (air masses, season, time of day, etc.) this parametrization is likely to be representative.

There might be other parameters ($[NO_x]$, [CO], local wind speed, UV radiation, etc.) that can be used to account for some of the variance in the *Gf* data. Ratios such as $[NO]/[NO_2]$ or benzene/toluene can be used to estimate the photochemical age of the air mass (Cubison et al., 2006). Of special interest are parameters that are also included in CTM and GCM so that the measured *Gf* variability can be directly compared to the corresponding values calculated by the models.

A description of $Gf(\mathrm{RH},d_\mathrm{d})$ would require H-TDMA observations at several relative humidities. While it is often useful to take most of the data at a high and fixed RH (RH = 90% commonly used), it is recommended that RH scans along the deliquescence branch are performed at least occasionally. The data should be examined for signs of deliquescence behaviour that might invalidate the use of continuous parametrizations of $Gf(\mathrm{RH},d_\mathrm{d})$ or $\varepsilon(d_\mathrm{d})$.

There is certainly a great interest in future studies of the efflorescence branch, for which there is practically no data for atmospheric aerosols. The existence of atmospheric aerosol particles in their metastable state at ambient conditions have only been observed in one H-TDMA study (Santarpia et al., 2004).

Ideally, not only $Gf(\mathrm{RH},d_\mathrm{d})$, but also the entire *Gf* probability density function *Gf*-PDF$(\mathrm{RH},d_\mathrm{d})$ should be described as succinctly as possible. The *Gf*-PDF can be constructed—for each pair of RH and d_d—from the results of a TDMAFit inversion of H-TDMA data by summing up each of the separable groups i of hygroscopic growth, normally distributed around their mean growth factors Gf_i with standard deviations σ_{Gfi} and number fractions AF_i. For a complete description, then also σ_{Gfi} and AF_i would need to be functions of RH and d_d, so that the entire *Gf* probability density function *Gf*-PDF$(\mathrm{RH},d_\mathrm{d})$ would be defined. In cases when *Gf*-PDF can be expected not to be a combination of normally distributed growth factors Gf_i, then the methods of Cubison et al. (2005) and Gysel et al. (2007) will have to be implemented. In practice, there are rarely sufficient H-TDMA data to support a complete *Gf*-PDF description, nor is it always necessary for the purpose for which the data were intended. Closure studies are often based on much simpler H-TDMA data sets, for instance $Gf(\mathrm{RH} = 90\%, d_\mathrm{d})$ combined with $AF_i(d_\mathrm{d})$, thus ignoring growth factor spread σ_{Gfi} and assuming that $\varepsilon(d_\mathrm{d})$ are constant over RH within the RH range under consideration (see Section 5.4).

3.8.3. Future atmospheric aerosol studies involving H-TDMA. The main feature of the TDMA technique is that it can be used to study the change in particle diameter resulting from any kind of aerosol processing, not merely humidification. The possibilities to employ the TDMA technique to gain chemical information for individual particles in the nucleation, Aitken and accumulation modes are most likely not yet fully explored.

Owing to its high inherent sensitivity in detecting and quantifying changes in particle diameter, the TDMA technique has a definitive advantage over competing methods for chemical analysis of individual particles smaller than ~100 nm in diameter. However, it suffers from the fact that the interpretation of TDMA data are not unambiguous when expressed in terms of chemical composition, and a firm theoretical link between the imposed aerosol processing and the resulting change in particle diameter has to be established and verified. For diameter changes due to water uptake, the theoretical framework exists today (see Section 5).

It may be possible to conceive TDMA systems employing aerosol processing in the form of selective chemical reactions to increase our understanding of the atmospheric aerosol. The principle behind such reaction R-TDMA systems was demonstrated as early as 1983 in a laboratory study of the reaction rate of sulphuric acid particles and gaseous ammonia (McMurry et al., 1983), in which the authors note that the resolution in diameter change was on the order of the thickness of a molecular monolayer.

Combinations of volatility and hygroscopicity (VH-TDMA) have shown promising results, at least when used in fairly simple atmospheric aerosol systems such as clean marine environments (Johnson et al., 2004a,b, 2005; Tomlinson et al., 2007) These combinations should be explored further.

As new and more sensitive particle sensors become available in the future, it may be possible to gain additional information regarding the physical and chemical nature of the particles belonging to each group of hygroscopic growth, by letting these sensors sample the aerosol exiting DMA2 instead of simply counting the particles using a CPC. Important properties that may be measured are the particle chemical composition, light scattering and absorbing properties, and cloud-nucleating properties. The sensors should be able to measure on individual particles or very small particle masses, and preferably work on-line. Off-line elemental and morphological analysis of aerosol particles separated with an H-TDMA is time consuming, and was demonstrated by McMurry et al. (1996).

In O-TDMA systems, the aerosol processing is performed by exposing the size-selected aerosol particles exiting DMA1 to an organic vapour, most often ethanol (Joutsensaari et al., 2001; Joutsensaari et al., 2004). The theoretical foundation for uptake of organic vapours is less developed than for water vapour, and chemical reactions, such as the formation of esters, may interfere with the analysis.

Multiple TDMA systems using various combinations of aerosol processing techniques in series, such as volatility followed by hygroscopicity (VH-TDMA), or even chemical reactions followed by hygroscopicity, may prove to be useful tools in

future aerosol studies. Data generated by several TDMA instruments operating in parallel (H-TDMA, V-TDMA and O-TDMA) are also likely to make important contributions to our knowledge of the atmospheric aerosol.

4. Growth factor parametrizations

Climate and air quality models describing the life cycle of atmospheric aerosols at various spatial and temporal scales need to incorporate a description of the size-resolved hygroscopic properties in some form. The various H-TDMA field data compiled here can be used to test the model predictions of hygroscopic behaviour in a variety of environments. Since the *Gf* data is given here only for RH = 90%, this H-TDMA data need to be parametrized in order to provide estimates of the *Gf* as function of RH in a wide range of RH commonly encountered in the troposphere. Several alternatives that can be derived from the general Köhler equation exist. A comprehensive summary of these parametrizations is given by Khvorostyanov (2007). An often used and very simple parametrization is

$$Gf = b(1 - \mathrm{RH})^{-\gamma}, \tag{4}$$

where γ is fitted to experimental H-TDMA data. Khvorostyanov (2007) shows that γ should be 1/3 for dilute particles obeying Raoults law. The dimensionless factor b accounts for the nature of the soluble material. Reported γ values are often smaller in magnitude (see for instance Swietlicki et al., 2000; Zhou et al., 2001; Massling et al., 2003).

Kreidenweis et al. (2005) derived another parametrization of *Gf* (RH) from the Köhler equation:

$$Gf = \sqrt[3]{1 + \left(a + b\,a_\mathrm{w} + c\,a_\mathrm{w}^2\right)\left(\frac{a_\mathrm{w}}{1 - a_\mathrm{w}}\right)}. \tag{5}$$

Here, the fitted parameters a, b and c are required to properly describe non-ideal solutions. Similar parametrizations were proposed by Brechtel and Kreidenweis (2000a, b). Rissler et al. (2006) proposed a simplification of this equation using only one parameter:

$$Gf = \sqrt[3]{1 + K\left(\frac{a_\mathrm{w}}{1 - a_\mathrm{w}}\right)}. \tag{6}$$

Since this latter formulation of *Gf* (RH) only contains one free parameter, it can be fitted to the measured *Gf* at RH = 90%, while eq. (5) requires *Gf* values to be measured for at least four RH.

The continuous one-parameter function approach can therefore make full use of existing H-TDMA data sets at RH = 90% such as those compiled here. What is gained in simplicity may however partly be lost in accuracy. The parametrization should therefore be tested whenever possible in a wider RH range to gain credibility, as was done in Rissler et al. (2006). Another requirement is that RH scans (humidograms) should not display any obvious step-like deliquescent behaviour.

The single parameter, K, may in some cases also be used to describe the critical supersaturation needed for activation. K should however not be derived from H-TDMA data taken at RH < 90% when intended for this purpose.

To further facilitate the use of H-TDMA data, K can be parametrized as a function of particle dry size, d_p, using relationships such as that suggested in Rissler et al. (2006),

$$K(d_p) = B\log(d_p) + C\,d_p + D, \tag{7}$$

where B, C and D are fitted parameters. In the derivation of eq. (6) from Köhler theory, the parameter K corresponds to

$$K = \phi(\eta)\kappa M_\mathrm{w}/\rho_\mathrm{w}, \tag{8}$$

where M_w and ρ_w are the molecular weight and density of pure water, and ϕ the osmotic coefficient, which is a function of the solution molality, η. For an ideal solution $\phi = 1$. The parameter κ represents the number of soluble moles of ions or molecules per unit volume dry particle, as suggested by Rissler et al. (2004, 2006). The soluble volume fraction, ε, can be used to represent the distribution of soluble ions over an aerosol particle size range, using a model salt. The two concepts are discussed in more detail in Rissler et al. (2008). κ and ε are related as:

$$\kappa = \varepsilon\,\rho_s\,\upsilon/M_s. \tag{9}$$

Here, ρ_s is the density of the model salt, υ the number of ions or dissolved molecules per molecule of the model salt, and M_s the salt molecular weight. The soluble volume fraction ε—often using ammonium sulphate as reference salt; ε_AS—has been widely used to relate H-TDMA growth factor data to the chemical composition of the aerosol particles.

We recommend that more and consistent studies are performed on the applicability and shortcomings of various growth factor parametrizations such as those mentioned here.

5. Theoretical consideration of chemical and physical properties influencing the hygroscopicity

5.1. The Köhler equation and its application to prediction of growth factor in subsaturated conditions

5.1.1. Water activity calculations. As seen from the Köhler equation (eq. 1), the water activity of the aqueous solution of the aerosol particle equals the water vapour saturation ratio (relative humidity) after correction for the effect of the solution surface curvature. Water activity, in turn, is linked to the chemical composition of the particle. Therefore, predictions of *Gf* at any given RH by necessity involves a model description of the water activity, a_w, of the solution. For ideal solutions, water activity obeys

Raoult's law,

$$a_{\mathrm{w}} = \frac{n_{\mathrm{w}}}{n_{\mathrm{w}} + n_s}, \tag{10}$$

where n_{w} and n_s are the moles of water molecules and dissolved ions or molecules in the solution, respectively. All real solutions below infinite dilution (i.e. below $a_{\mathrm{w}} = 1$), deviate from an ideal behaviour, to a greater or lesser degree. There are a large number of potential methods to predict water activity for non-ideal solutions, depending on the components present in the particle. For inorganic electrolytes, the most accurate are ionic interaction models, with those calculating activities on a mole fraction basis being most capable of accurate representation of component activities at lower RH (up to concentrations of 40 Mol kg^{-1} solute concentration, e.g. (Wexler and Clegg, 2002), online model: http://www.aim.env.uea.ac.uk/aim.htm). Ion interaction models on a molality scale are available for a wider range of electrolytes, but only to lower concentrations (e.g. the Pitzer model is valid up to 6 Mol kg^{-1}) and hence are unsuitable for evaluating component activities at lower than around 90% RH. The solute activities in such models can explicitly account for higher order than fundamental binary interactions, or may use simple mixing rules (such as Bromley's method or that of Kusik and Meissner). The water content, too, can be solved by accounting for the ionic interactions (solving the water equation within the energy minimization) or can be evaluated by use of relationships derived from mixing rules (such as that of Zdanowskii, Stokes and Robinson (ZSR), (Zdanovskii, 1948; Stokes and Robinson, 1966). This is treated in Section 5.2 below. Whichever method is used to evaluate multicomponent water content, the prediction must include the water associated with all components. Such binary aqueous solution data may be readily available for inorganic systems of atmospheric importance, but are seldom available for atmospherically representative organic compounds. This necessitates the use of models to predict the water activity in the aqueous organic solution. There are a number of approaches which have been used, from explicit considerations of compound interactions [e.g. extended ZSR approach of (Clegg and Simonson, 2001)], to empirically fitted approaches [such as UNIQUAC used in (Ming and Russell, 2002)] and more generalized group contribution techniques such as UNIFAC (as used in Topping et al., 2005b). Various developments have been made to UNIFAC in order to most appropriately treat atmospherically relevant components through development of new group interaction parameters (e.g. Peng and Chan, 2001), based on emerging laboratory data. The contribution to the water content by a number of organic components may be directly evaluated within the organic activity coefficient model, and combined with the water associated with the inorganic components in a coupled model (see figures 3 and 7 in Topping et al., 2005b). Such models may (e.g. Ming and Russell, 2002) or may not (Topping et al., 2005b) explicitly account for interactions between inorganic and organic solutes. Alternatively, the contributions may be lumped and treated in an additive manner as described in Section 5.2 for the ZSR method.

5.1.2. Surface tension effects. The surface tension enters the Kelvin term of the Köhler equation (eq. 1), which becomes important at high RH (and at supersaturation) and at small particle sizes. Since the Kelvin term is exponentially dependent on the particle surface tension, the requirement to capture the various multicomponent particle properties varies in degree of accuracy in different regimes. Owing to the relatively minor influence on surface tension of inorganic electrolytes, it is unnecessary to develop complex parametrizations to capture surface tension effects in evaluating the Kelvin factor in such systems. However, the atmospheric aerosol may contain many hundreds or even thousands of organic components. Given the variety of mixing states of ambient aerosol, it may be inferred that individual particles may contain a large number of organic components. It is well known that certain classes of organic compounds will reduce the surface tension of an aqueous solution below that of pure water. Even ignoring the explicit partitioning of surface active components between the surface layer and bulk interior of the particle (discussed below), the prediction of surface active effects can be done at many levels of complexity, from using 'two-dimensional' group interaction models to application of simpler mixing rules. The sensitivities of *Gf* predictions to various approaches in subsaturated conditions has been investigated in (Topping et al., 2005b) and in supersaturated conditions in (Topping et al., 2007) and (Rissman et al., 2007). The magnitude and direction of the contribution of inorganic electrolytes on surface tension in mixed systems is highly composition dependent (see Topping et al., 2007); thus inorganic contributions cannot be neglected a priori in such systems. The sensitivity to the surface tension model choice is more important with decreasing dry size and increasing RH, since these are the conditions where *Gf* is most sensitive to the Kelvin factor. Owing to the reduced dependence of the surface tension on the Kelvin term in subsaturated conditions (when compared with the huge dependence in cloud activation), it has been frequently ignored in calculating the *Gf* from composition. With decreasing size, the Kelvin term is typically calculated using the surface tension of pure water. A number of empirically found relationships have been reported to relate surface tension to concentration of carbon (see e.g. Facchini et al., 1999); but these have been used most widely in predicting the effect of organic compounds on cloud activation. A full consideration of the effect of organic components on multicomponent aerosol surface properties has not been reported. It may be expected that such effects will be important in H-TDMA studies of nucleation mode particles ($< \sim$20 nm) in particular and should be a focus of future work.

A complication when considering surface tension is the tendency of surface active molecules, by definition, to partition to the surface of an aqueous particle. For large systems, the bulk concentration can be calculated from the total moles of the substances involved as the amount of surfactant in the surface layer

is a negligible fraction of its total amount in the system. However, for small systems with a high surface-to-volume ratio the situation is different, and depending on the degree of surface activity of the component, the partitioning of the surfactant between the bulk and the surface has to be accounted for when calculating the bulk concentration from given total numbers of moles. The effect on cloud activation predictions by consideration of the equilibrium of water vapour with growing aerosol particles was explored first by Li et al. (1998) who demonstrated that, while critical supersaturation S_{crit} was lowered by the surface tension in pure sodium dodecyl sulphate (SDS) particles, in NaCl/SDS particles, S_{crit} was raised by replacement of small NaCl with larger SDS molecules. Sorjamaa et al. (2004) demonstrated that consideration of surface to volume partitioning should be included in the Raoult term and that the resulting S_{crit} could be higher than just considering the surface tension of water. Kokkola et al. (2006) demonstrated that this was also true for atmospherically representative organic compounds. Topping et al. (2005a), further extended this approach to consider multiple surfactant species. It is currently unclear whether the consideration of surface partitioning improves agreement in all cases (Rissman et al., 2007). Furthermore, a systematic comparison of the effects of surface partitioning in the calculation of subsaturated growth factor with measured values has not been reported. Such impacts under the lower water concentration (and correspondingly high surfactant concentration) conditions should be explored.

5.1.3. Other Parameters (partial molar volume, solution density, dry density). By inspection of the Köhler equation, it is clear that parameters other than water activity and surface tension also play a part in the growth of particles in the humid atmosphere.

5.1.3.1. Partial molar volume. It can be seen in the Köhler equation that the Kelvin term is exponentially dependent on the partial molar volume of water (ν_{w}) in the growing particle. Shulman et al. (1996) and Chylek and Wong (1998) both substituted ν_{w} with the quotient of the molecular weight of water (M_{w}) and the solution density (ρ_{sol}). Kreidenweis et al. (2005) demonstrated how this leads to inaccurately low ν_{w}. The formal expression of partial molar volume of water contains a term describing the derivative of solution density with respect to mass fraction of solute ($\mathrm{d}\rho_{\mathrm{sol}}/\mathrm{d}x$). However, it was demonstrated by Brechtel and Kreidenweis (2000b), that the volume additivity assumption (partial molar volume equals the molar volume) introduces insignificant errors in ν_{w} through droplet activation such that the ν_{w} may be replaced with the quotient of the M_{w} and the water density (ρ_{w}) with negligible error. When using this approximation under more concentrated solutions (i.e. under subsaturated conditions) significant deviation can be introduced even for inorganic salt solutions. Insufficient data exist to calculate the partial molar volume for most atmospherically realistic particles and it is necessary to systematically investigate the errors introduced by the volume additivity assumption for multicomponent inorganic/organic solutions for which there are data.

5.1.3.2. Solution density. Although the solution density does not enter into the Köhler equation through the partial molar volume (see Section 5.1.3.1), it is needed to calculate particle wet volume and hence growth factor. There are a number of mixing rules and approximations that can be used. Simple combination rules have been reviewed in the literature (e.g. Tang, 1997) and it has been found that mixed solution density can be calculated using only the binary solution data using the following rule:

$$\frac{1}{\rho_{\mathrm{sol}}} = \sum_i \frac{X_i}{\rho_{o,i}}, \tag{11}$$

where X_i is the dry solute mass fraction for compound i and ρ_{oi}, is the binary solution density for compound 'i' at the solute concentration of the mixture. The mass fraction mixing rule, also consistent with the assumption of volume additivity, has been found to be more accurate than replacing the mass fraction by the mole fraction for a number of inorganic systems; though this has not been demonstrated for organic systems. For inorganic systems, the growth factor difference associated with the two separate mixing rules is likely to be within any experimental uncertainty associated with the H-TDMA.

For inorganic solutions the binary data is available in the literature (e.g. Cohen et al., 1987b, c; Tang, 1997; Jacobson, 1999). When binary organic data is not available it can be calculated using the same rule given above. While some studies in the literature use the solid organic density for this purpose, it is possible to calculate the supercooled liquid density of the organic component using the Yens-Wood method (Yens and Woods, www.pirika.com).

5.1.3.3. Dry density. As with the solution density, the particle component dry density does not enter into the Köhler equation but is necessary to calculate growth factor. It is necessary to assume the physical state of the dry particle when calculating the dry density. A sensitivity analysis of the assumptions for some inorganic systems is presented in (Topping et al., 2005b) and for organic systems in (Topping et al., 2005a). In certain cases the sensitivity should be resolvable using H-TDMA instruments.

5.2. The applicability of the ZSR mixing rule

Atmospheric aerosol particles each contain a multitude of chemical compounds, which is manifested also in their hygroscopic properties as measured by H-TDMA instruments. Considering the complexity of ion interaction models and the difficulties to adequately characterize the fully size-resolved aerosol chemical composition, there is a need for simpler model approaches that

can be implemented more easily on atmospheric aerosol data sets.

The ZSR mixing rule is based on the assumption that the water content from individual components are additive, so that the total amount of water contained in an aerosol particle can be estimated by summing the water taken up by all components as if they were totally independent of each other. One formulation of the ZSR method mixing rule is therefore

$$\text{mass}_{\text{water\_tot}} = \sum_i \text{mass}_{\text{water\_}i}, \tag{12}$$

where $\text{mass}_{\text{water\_tot}}$ is the mass of water in the mixture at the given water activity and $\text{mass}_{\text{water\_i}}$ is the mass of water that would have been associated with the amount of the single electrolyte *i* present in the mixed particle at the same water activity.

In recent years there has been considerable interest in using simplifying assumptions to predict hygroscopic growth factors. The most widely used treatment was that pioneered by Malm and Kreidenweis (1997), which sought to express the growth factor of particles in terms of the growth factor of individual components all at the same water activity by making use of the ZSR assumption. The convenient form of the ZSR mixing rule expressed in terms of *Gf* is:

$$Gf_{\text{mixed}}(a_w) = \left\{ \sum_{i=1}^{n} \varepsilon_i \left[Gf_i(a_w) \right]^3 \right\}^{1/3}. \tag{13}$$

The individual component growth factors $Gf_i(a_w)$ may either be directly measured in laboratory experiments or predicted from appropriate models. It is then possible, by making appropriate assumptions about mixing state and the multicomponent particle density, to use measurements of aerosol component mass to calculate the component volume fractions, ε_i, and evaluate the mixed particle growth factors, Gf_{mixed}. Insoluble particle volume fractions are treated using $Gf = 1$. The terms are all evaluated at the same water activity, a_w, approximated by conducting the measurements/calculations at the same RH. The size-dependence of *Gf* enters in applying the Kelvin curvature correction when calculating a_w from RH. The Gf_{mixed} values may then be compared with directly measured growth factors to quantify the understanding of the system behaviour. Such hygroscopic closure studies will be discussed in Section 5.4 below.

There has been no systematic comparison between particle water content calculated using explicit thermodynamic models and by use of 'additivity' assumptions. In general, this is difficult since insufficient fundamental data exist to construct the thermodynamic relationships to model multicomponent aerosol (with particular regard for inorganic/organic interactions). It is, however, possible to compare predicted water content for limited systems where such data are available. One such comparison between a thermodynamic model and the ZSR method for electrolyte solutions containing NH_4^+, Na^+, H^+, SO_4^{2-}, NO_3^- and Cl^- (neglecting the effects of curvature) is given in (Topping et al., 2005a) (their Table 3). As one might expect, when moving away from ideality with reducing RH the discrepancy increases, since the ZSR assumption ignores solute/solute interactions. For the ternary electrolyte solutions the deviation is not usually greater than 2% and will result in a *Gf* difference of 0.01 or so—well within the uncertainty of H-TDMA instruments. However, for the four electrolyte solutions, the discrepancy can be higher than a *Gf* difference of 0.05 and should be detectable by H-TTDMA measurements. In the real atmosphere, the aerosol particles are likely to contain a very high number of components so reliance on mixing rules which depend solely on binary data is not guaranteed to be sufficiently accurate. For mixed systems, Choi and Chan (2002a, b) found that the effects of glycerol and of malonic, succinic, glutaric and citric acids on the water cycle of NaCl and $(NH_4)_2SO_4$ was reasonably well explained using the ZSR assumption. Svenningsson et al. (2006b), on the other hand, observed large deviations from the ZSR mixing rule for their MIXSEA mixture of NaCl, $(NH_4)_2SO_4$, succinic acid and fulvic acid.

This is an example of the fact that the choice of the binary system for input to the mixing rule can affect the ZSR predictions, as was discussed for similar systems in Section 3.3 above. Here, the ZSR predictions of water uptake hinge upon whether the dry state of the inorganic compounds is defined as being a mixture of NaCl–$(NH_4)_2SO_4$ or NH_4Cl–Na_2SO_4. The dry density of the particles—and thereby dry particle volume—may also depend on the type of salts formed during crystallization. While the explicit thermodynamic models will handle the water uptake appropriately once all ions are in solution, they still suffer from a poorly defined dry state when used to predict volume-based growth factors as measured by the H-TDMA. See Section 5.2.1 below.

Other studies have used the ZSR technique to explain water uptake in solutions of carboxylic, dicarboxylic and multifunctional acids with one electrolyte with varying success (Hansson et al., 1998; Cruz and Pandis, 2000; Hameri et al., 2002; Chan and Chan, 2003). Topping et al. (2005b) find that the use of the ZSR assumption for mixtures of five carboxylic acids and each of three separate inorganic electrolytes resulted in very good agreement at high relative humidities but, at low RH (~40%), underpredicted water content in NH_4NO_3-containing solutions while overpredicting water content in the mixed solutions containing either NaCl or $(NH_4)_2SO_4$. Ming and Russell (2002) briefly investigated the discrepancy between the ZSR assumption and explicit thermodynamic calculation of water content in a number of mixed inorganic/organic systems. In general the difference was not usually greater than 3%, but for systems including highly soluble organic acids the deviation could be as high as 10%. It should be noted that the extrapolation of interaction parameters between systems can be worse than assuming additivity, and use of the ZSR assumption may predict values closer to those measured than inappropriate estimation of solute interactions.

It would be desirable to conduct a systematic comparison of different degrees of complexity of modelling approaches against measurements for a range of mixtures for which there are fundamental data to construct explicit thermodynamic models.

5.2.1. Correct ion pairing when using the ZSR assumption. Obviously the water content per unit mass of material predicted by the ZSR mixing rule may be sensitive to the electrolytes resulting from the chosen ion pairing if their dry or solution properties are sufficiently different to produce significantly different pure component growth factors. It is necessary to choose an appropriate methodology for ion pairing before application of the ZSR mixing rule to inorganic electrolytes. Such an ion-pairing algorithm defining appropriate equivalent concentrations of electrolytes is reported in Reilly and Wood (1969), and has been reported by Clegg and Simonsen (2001), Clegg et al. (2003) and Topping et al. (2005b) as an appropriate and recommended method for ion pairing when using the ZSR technique in predicting aerosol water. Use of equivalent concentration provides a thermodynamically defensible method for ion-pairing which an arbitrary pairing cannot.

An alternative technique was reported by Gysel et al. (2007). In this study the goal of ion pairing was to find a set of neutral salts, with as little computational effort as possible, such that the corresponding ZSR prediction gives best possible agreement with a full thermodynamic model prediction of water uptake for given numbers of anions and cations. Since the compositions as a function of size were well determined in this study, the ion pairing choice could be constrained in a computationally efficient tractable manner. In the absence of such compositional constraint, it is recommended that the Reilly and Wood (1969) scheme is used when applying the ZSR assumption in atmospheric applications.

5.3. The effects of deliquescence

Pure compounds such as inorganic salts are well known to display an RH hysteresis behaviour. When increasing RH from a low value, the aerosol particles remain in a dehydrated state—where only the particle surface is wetted—until the RH (water activity) is reached at which the solubility of the compound allows for the formation of a saturated aqueous solution. This is the RH of deliquescence (DRH) and is readily observed as an abrupt increase in particle diameter. Increasing the RH further will cause the particle to take up more water and grow in accordance with the Köhler equation (eq. 1). When decreasing RH below the point of deliquescence, the solution will in many cases become supersaturated with respect to the solute and attain a metastable state which can only exist in the suspended aerosol particles. Only at a much lower RH—the RH of efflorescence—a solid phase will again form causing the particle to shrink to its original dehydrated size.

For particles consisting of compounds with different DRH, the less soluble compound will gradually dissolve in the aqueous solution provided by the more soluble compound, resulting in a smooth diameter growth with increasing RH instead of a stepwise deliquescence behaviour. In its extreme, the gradual dissolution of a multitude of compounds (Marcolli et al., 2004) will smear out all deliquescence behaviour and result in a smooth and continuous particle water uptake with changing RH, both for increasing and decreasing RH.

Indications of deliquescence behaviour with increasing RH has been observed in only a few H-TDMA studies of atmospheric aerosols (Berg et al., 1998b; Santarpia et al., 2004), while others find an apparent lack of deliquescence (Pitchford and McMurry, 1994; Zhou et al., 2001; Rissler et al., 2006; Sjogren et al., 2007a). We are only aware of one H-TDMA study that has observed the full RH hysteresis behaviour in atmospheric aerosols (Santarpia et al., 2004). The authors used an intricate humidification system to enable them to demonstrate the existence of metastable particles. There is a clear need for more H-TDMA studies characterizing the water uptake in a wide range of RH, since this is of utmost importance for the direct effect of aerosol on climate and visibility reduction.

Theoretical treatment of deliquescence is straightforward for inorganic electrolytes and their mixtures for which data are available, with prediction of stepped deliquescence of complex salts readily possible (see fig. 4 in Topping et al., 2005b). The predicted size dependence of deliquescence is also readily predictable and should be detectable with H-TDMA instruments. Biskos et al. (2006) demonstrated that H-TDMA-measured growth factors of NaCl particles between 6 and 60 nm diameter steadily decreased within detection limit for dry sizes below 40 nm with an increase in the *DRH* with decreasing dry size. It has yet to be shown whether this behaviour can be resolved for other salts and mixed salts.

It is the norm to consider the transition from an uncoated dry aerosol to a dissolved salt droplet. However, several studies have shown that it may be more suitable to consider the transition from a wetted particle to a dissolved droplet (Ghosal and Hemminger, 1999; Weis and Ewing, 1999; Finlayson-Pitts and Hemminger, 2000). Mirabel et al. (2000) developed a model to predict the prompt deliquescence, and its dependence on particle size, for a generic crystal with an ideal solution. More recently, Russell and Ming (2002) developed a similar model for treating wetted particles and non-ideal effects. Topping et al. (2005a) found that while the lack of any change in *DRH* for the sub 100 nm $(NH_4)_2SO_4$ aerosol studied by Hameri et al. (2000) is an interesting result, both ADDEM (Topping et al., 2005a, b) and the model of Russell and Ming (2002) predict an increase should occur. The latter authors probed the sensitivity to the calculated *DRH* point for various values of the surface tensions of the solid–vapour and solid–liquid interface. They found that it is possible that a wetted particle may be more stable than the aqueous solution, thus increasing the *DRH* point. Unfortunately, knowledge of surface tensions of crystalline structures is limited and it is unlikely that data is available for mixed inorganic/organic particles.

Suppression of solid phase precipitation in detailed models can be used to calculate metastable solutions for direct comparison with the ZSR curves. Following this 'efflorescence arm' of the particle is possible for H-TDMA systems and predictions can be tested by such measurements.

It is also possible to predict the RH at which dissolution will occur for organic compounds for which the solid energy of formation is known. Fig. 2 in Topping et al. (2005b) demonstrates such prediction for multiple carboxylic acids in solution. The situation is more complex for mixtures of inorganic electrolytes with organic compounds resulting from the lack of experimental data. Consideration of atmospherically representative mixed aerosol is therefore not possible. Efflorescence (the onset of crystallization) is a stochastic process that can be predicted by various nucleation theories with differing degrees of success. The theoretical methodology exists for a more complete H-TDMA study of the effects of deliquescence and efflorescence.

5.4. Reconciliation of H-TDMA measurements with composition and cloud activation behaviour

A number of 'closures' between particle hygroscopicity and other measured properties are possible. Such studies involve quantification of the degree of reconciliation of the measured growth factor at a given humidity (or at a range of humidities) with the measured property of interest using explicit or parametrized relationships (Quinn et al., 1996). The most useful and widely attempted closure studies fall into two classes:

(1) The prediction of growth factor from measured composition for comparison with H-TDMA-measured growth factor, and

(2) The prediction of cloud activation properties from H-TDMA-measured growth factor for comparison with critical supersaturation (S_{crit}), activated fraction (F_A) or diameter of particle at which 50% of the aerosol population are activated (D_{50}) measured using a cloud condensation nucleus (CCN) counter.

Both classes of study can be conducted in the laboratory or in the ambient atmosphere, with the former providing a more constrained set of conditions and consequently greater ability to test the method used to attain closure. The degree of external versus internal mixture must be taken into account in these studies. It is not the intention to review all possible closure studies, only to illustrate the variety of techniques employed.

5.4.1. Composition/hygroscopicity closure on field data. There are a large number of methods which can be used to establish the composition and mixing state of a population of aerosol particles with a wide variation in the information available. Using an appropriate choice of the techniques described above it is then possible to attempt to compare the *Gf* predicted from these measurements with that measured by H-TDMA instruments. The most straightforward closure is that which relies on the least detailed compositional information. Broad measurements of aerosol composition are available online from modern instrumentation such as the Aerodyne Aerosol Mass Spectrometer (AMS). Such instruments can provide high temporal resolution of size segregated composition, but with little detailed chemical information, particularly for the organic components. By making simplifying assumptions about the physical behaviour of the various fractions, it is possible to use water content mixing rules such as the ZSR assumption to predict the *Gf* at any RH for which individual component *Gf* is known or can be approximated.

The earliest attempts at composition/hygroscopic closure used impactor measurements of composition and limited offline analyses. H-TDMA and impactor data from Grand Canyon and Los Angeles were used by Saxena et al. (1995) to infer that organic material affected ambient aerosol hygroscopic properties; organic components in freshly produced aerosol particles hindering water uptake, while those in aged air masses increasing growth. Swietlicki et al. (1999) used Berner impactor/ion-chromatography determinations of inorganic ions to predict H-TDMA-measured hygroscopicity at Great Dun Fell, in 1995. The hypothesized model used water activity data for ammonium sulphate to calculate soluble volume fraction and hence predict the number of ions in the appropriate impactor size fraction. It was found that the inorganic components measured in 0.17–0.53 μm diameter particles could explain the measured water uptake within measurement and model uncertainties for all cases but one, for which the contribution of organic oxygenated substances to water uptake was invoked.

The first more tangible evidence that organic compounds contribute significantly to the water uptake of atmospheric aerosols was presented by Dick et al. (2000). They observed higher hygroscopic *Gf* using an H-TDMA than predicted by the inorganic compounds and applying the ZSR mixing rule. The discrepancy between observed and predicted water uptake clearly increased with increasing organic aerosol mass fraction. Water uptake at low RH, which is often observed for atmospheric particles, was attributed primarily to organics.

Gysel et al. (2004) conducted an investigation into the impacts of the less hygroscopic fraction (ISOM) of the water-soluble organic matter (WSOM) in rural ambient samples from K-puszta, Hungary. The ISOM, which constitutes the major fraction of WSOM, deliquesced between 30 and 60% RH, and hygroscopic growth factors at 90% RH ranged from 1.08 to 1.17. The hygroscopic behaviour of investigated fulvic and humic acids had similarities to ISOM, but hygroscopic growth factors were slightly smaller and deliquescence was observed at higher RH (75–85% and 85–95% RH for fulvic acid and humic acid, respectively). The hygroscopicity of the smaller remaining mass of the 'most' hydrophilic organic matter (MHOM) was used as a tuner in the closure (using the ZSR assumption) with H-TDMA measurements, but remained the largest uncertainty in the modelling exercise. Good agreement between model prediction and

measured water uptake was observed only by inclusion of the water associated with the MHOM.

Mircea et al. (2005), using a modified form of the Köhler equation, demonstrated that, in order to predict *Gf* of wet and dry season Amazonian samples which are dominated by organic components, it is necessary to know the solubility of WSOC (this contrasts with the ability to predict CCN behaviour which did not require such information).

McFiggans et al. (2005) used a detailed thermodynamic model to predict the *Gf* of aerosol sampled in polluted continental air using compositional measurements provided by mapping the detailed speciation of inorganic and organic components from impactors onto highly size-resolved aerosol mass spectrometer mass distributions. It was found that very good agreement with H-TDMA-measured *Gf* when appropriate sample averaging was carried out, and when measured *Gf* did not vary significantly across each impactor sampling period. In addition, it was found that there was a relative insensitivity to the representation of the organic fraction. The organic components had a *Gf* close to 1.1 at 90% RH irrespective of air mass history. The particle hygroscopicity variability was dominated by the inorganic:organic ratio.

Aklilu et al. (2006), used highly time- and size-resolved AMS data from the Pacific 2001 field study and obtained reasonable agreement with H-TDMA measurements under conditions when the dominant inorganic component was sulphate, with poorer agreement under nitrate-rich conditions. Their claim is that '... the ZSR mixing rule fails for nitrate'. It is unlikely that the mixing rule is at fault and it may be more appropriate to state that an attribution of AMS-observed nitrate to NH_4NO_3 in ZSR calculations may be incorrect. Alternatively, such observations are consistent with the observation reported in (Swietlicki et al., 1999) that nitrate evaporation in DMA1 was possible for acidic aerosol as has been reported in (Berg et al., 1998a). The possibility of such a nitrate artefact was also evident in the closure study of Gysel et al. (2002).

Recommendations: For composition—hygroscopicity closure, measurements of composition and mixing state need to be made at the same time resolution as the comparison *Gf* measurements so that they may be compared with the *Gf* predictions. It would be useful to make predictions of the multicomponent particle *Gf* as a function of RH for comparison with humidograms over the same time period. It is difficult to identify how compositional measurements can be made available at a sufficient level of specificity for detailed thermodynamic modelling at the resolution of the H-TDMA measurements. In such cases, composition and hygroscopicity should be sampled or averaged appropriately with a sufficient uncertainty analysis. There is encouraging closure obtained in recent studies using simple additivity mixing rules. A thorough comparison should be conducted between such simplifications and more detailed predictive methods prior to recommending widespread adoption, but use of such tools could prove to be a valuable and efficient route forward.

5.4.2. Hygroscopicity—CCN closure. There are a number of studies that have aimed to quantify the subset of aerosol particles acting as cloud condensation nuclei (CCN) and relate these to the aerosol hygroscopic properties. Some of those that have employed H-TDMA measurements are summarized in table 6 of McFiggans et al. (2006). Recently there have been significant developments in the theoretical tools to link measurements made in the sub and supersaturated regimes. This Section focuses on several closure studies which have employed such approaches.

Brechtel and Kreidenweis (2000b) presented a theoretical framework to predict critical supersaturation by inserting two parameters (Y_f and $\beta_{0,f}$) fitted to H-TDMA measurements into a simplified functional form for the osmotic coefficient in the Köhler equation. They found that three diameter/RH data pairs between 80 and 92% RH were capable of giving the same accuracy in prediction of S_{crit} as ten data pairs over the same region for inorganic electrolytes. The model was applied to laboratory and ambient data in (Brechtel and Kreidenweis, 2000a). It was found that single salt H-TDMA measurement-derived S_{crit} and theoretical values differed on average by –13% but that comparisons with CCN counter derived measurements on ambient particles of unknown composition were in greater error (–6 to –65%).

Dusek et al. (2003) used a simplified form of the Köhler equation to calculate CCN spectra from H-TDMA measurements made during the ACE 2 project. Their model approach overestimated the measured CCN concentrations by 30%.

Vestin et al. (2007) achieved closure between predicted and measured CCN concentrations over a range of supersaturations, within the combined errors of model and measurements (slight underprediction by 15–20%). The predictions were based on the H-TDMA *Gf* data at RH = 90% from which the single parameter *K* (eqs. 6 and 8) was determined.

Kreidenweis et al. (2005) and Koehler et al. (2006) reported the development of the three-parameter form of the so-called κ-Köhler theory referred to in Section 4 (eq. 5) for inorganic-only and organic-containing aerosol, respectively. Reasonable comparisons with critical supersaturation and critical dry diameter made using other models and directly with measurements for NaCl and $(NH_4)_2SO_4$ were achieved, provided H-TDMA-derived a_w was 'corrected' or adjusted adequately for the Kelvin term and the dry particle shape factor was adequately treated. H-TDMA-measurement derived critical dry diameters at between 0.2 and 1% supersaturation were within experimental error of previously reported measured values for glutaric, malonic and oxalic acids and levoglucosan.

In hygroscopicity—CCN closure studies where the objective is to extrapolate the hygroscopic behaviour to supersaturation, the H-TDMA should be operated at a RH that is as high as possible without endangering *Gf* accuracy and precision (RH = 90% or higher). In composition—hygroscopicity closure studies, it may be more relevant to study also the hygroscopic properties at humidities lower than RH = 90% in order to capture the

non-ideal behaviour of the solution. Since the same H-TDMA data set is often used in both these types of closure studies as well as for process-type studies (for instance Mircea et al., 2005; Rissler et al., 2006; Vestin et al., 2007), compromises have to be made to ensure that adequate time and (dry) size resolution can be maintained when adding more DMA2 humidities to the H-TDMA measurement schedule. In studies where the aerosol chemical composition can be obtained with high time resolution using for instance an AMS, then a high time resolution is likely to be preferred to the alternative of gaining additional information on *Gf* (RH).

5.5. Summary and recommendations

A full consideration of the effect of organic components on multicomponent aerosol surface properties including surface-bulk partitioning has not been reported. It may be expected that such effects will be important in nano-H-TDMA studies in particular and should be the focus of future work.

There has been no systematic comparison between particle water content calculated using explicit thermodynamic models and by use of 'additivity' assumptions. It would be desirable to conduct a systematic comparison of different degrees of complexity of modelling approaches against measurements for a range of mixtures for which there are fundamental data to construct explicit thermodynamic models.

The theoretical methodology exists for a more complete H-TDMA study of the effects of deliquescence and efflorescence.

There is a specific need to examine the sensitivity of predicted *Gf* as a function of RH on molecular structure, molecular weight, functionality and other properties. This needs to be compared with a systematic H-TDMA laboratory study across a wide range of organics.

There is a requirement to quantify how well closures at different degrees of complexity explain the observations—that is, we need a definition of the 'skill' of the closure attempts—when do we really have closure?

6. Conclusions

H-TDMA instruments have been used successfully over the last two decades to determine the hygroscopic properties of atmospheric aerosol particles in a variety of environments around the globe. The available H-TDMA data enable us to draw firm conclusions regarding the characteristic hygroscopic behaviour of aerosol particles in marine, rural and urban environments as well as for nucleation mode particles. The interpretation and intercomparison of the H-TDMA data is greatly facilitated by a classification of the observed hygroscopic growth factors into nearly hydrophobic, less-hygroscopic, more-hygroscopic and sea salt particles. There is nevertheless still a great need for additional H-TDMA data representative for several continental regions, in particular in Africa and Asia, as well as for free tropospheric aerosols. Furthermore, most of the H-TDMA data is taken at only one RH (often 90%), making it difficult to draw firm conclusions regarding the behaviour at lower RH, which may involve deliquescence and the existence of metastable states.

The time scales for atmospheric processes transforming freshly emitted nearly hydrophobic particles into less-hygroscopic and eventually more-hygroscopic aerosol particles are not well understood and should be studied further.

The hygroscopic properties carry information about the sources and atmospheric processes shaping the atmospheric aerosol and its physical and chemical properties. Models should be able to reproduce these properties, and H-TDMA data are thus useful as a tool for model evaluation.

Extrapolations of H-TDMA data to water vapour supersaturation have in many cases been shown to provide accurate predictions of the CCN activity of the aerosol. There are nevertheless still many remaining issues to tackle, in particular regarding our ability to link aerosol particle chemical composition with the hygroscopic and CCN properties. It has only recently become evident that organic aerosol compounds contribute significantly to the water uptake. The intricate interplay between inorganic and organic compounds, including surface tension effects, remains to be elucidated. These interactions and processes need to be parametrized to enable them to be properly handled in global and regional air quality and climate models that include an explicit description of the size-resolved chemical composition.

Considering the vital importance that hygroscopicity has on the direct and indirect effects on climate, it is clear that H-TDMA instruments have a very important role to play in future atmospheric aerosol studies.

7. Acknowledgments

This work was carried out within the frameworks of the EU FP6 Integrated Project EUCAARI, the EU FP6 Infrastructure Project EUSAAR as well as the NOS-N Nordic Centre of Excellence BACCI.

References

Aklilu, Y., Mozurkewich, M., Prenni, A. J., Kreldenweis, S. M., Alfarra, M. R. and co-authors. 2006. Hygroscopicity of particles at two rural, urban influenced sites during Pacific 2001: comparison with estimates of water uptake from particle composition. *Atmos. Environ.* **40**, 2650–2661.

Aklilu, Y. A. and Mozurkewich, M. 2004. Determination of external and internal mixing of organic and inorganic aerosol components from hygroscopic properties of submicrometer particles during a field study in the Lower Fraser Valley. *Aerosol. Sci. Tech.* **38**, 140–154.

Andreae, M. O., Charlson, R. J., Bruynseels, F., Storms, H., Vangrieken, R. and co-authors. 1986. Internal mixture of sea salt, silicates, and excess sulfate in marine aerosols. *Science* **232**, 1620–1623.

Baltensperger, U., Streit, N., Weingartner, E., Nyeki, S., Prevot, A. S. H. and co-authors. 2002a. Urban and rural aerosol characterization of summer smog events during the PIPAPO field

campaign in Milan, Italy. *J. Geophys. Res.-Atmos.* **107**, 8193, doi:8110.1029/2001JD001292.

Berg, O. H., Swietlicki, E., Frank, G., Martinsson, B. G., Cederfelt, S.-I. and co-authors. 1998a. Comparison of observed and modeled hygroscopic behaviour of atmospheric particles. *Contr. Atmos. Phys.* **71**, 47–64.

Berg, O. H., Swietlicki, E. and Krejci, R. 1998b. Hygroscopic growth of aerosol particles in the marine boundary layer over the Pacific and Southern Oceans during the First Aerosol Characterization Experiment (ACE 1). *J. Geophys. Res.-Atmos.* **103**, 16535–16545.

Biskos, G., Malinowski, A., Russell, L. M., Buseck, P. R. and Martin, S. T. 2006. Nanosize effect on the deliquescence and the efflorescence of sodium chloride particles. *Aerosol. Sci. Tech.* **40**, 97–106.

Brechtel, F. J. and Kreidenweis, S. M. 2000a. Predicting particle critical supersaturation from hygroscopic growth measurements in the humidified TDMA. Part II: laboratory and ambient studies. *J. Atmos. Sci.* **57**, 1872–1887.

Brechtel, F. J. and Kreidenweis, S. M. 2000b. Predicting particle critical supersaturation from hygroscopic growth measurements in the humidified TDMA. Part I: theory and sensitivity studies. *J. Atmos. Sci.* **57**, 1854–1871.

Busch, B., Kandler, K., Schutz, L. and Neususs, C. 2002. Hygroscopic properties and water-soluble volume fraction of atmospheric particles in the diameter range from 50 nm to 3.8 μm during LACE 98. *J. Geophys. Res.-Atmos.* **107**, 8119, doi: 8110.1029/2000JD000228.

Buzorius, G., McNaughton, C. S., Clarke, A. D., Covert, D. S., Blomquist, B. and co-authors. 2004. Secondary aerosol formation in continental outflow conditions during ACE-Asia. *J. Geophys. Res.-Atmos.* **109**, D24203, doi:10.21029/22004JD004749.

Carrico, C. M., Kreidenweis, S. M., Malm, W. C., Day, D. E., Lee, T. and co-authors. 2005. Hygroscopic growth behaviour of a carbon-dominated aerosol in Yosemite National Park. *Atmos. Environ.* **39**, 1393–1404.

Cavalli, F., Facchini, M. C., Decesari, S., Emblico, L., Mircea, M. and co-authors. 2006. Size-segregated aerosol chemical composition at a boreal site in southern Finland, during the QUEST project. *Atmos. Chem. Phys.* **6**, 993–1002.

Chan, M. N. and Chan, C. K. 2003. Hygroscopic properties of two model humic-like substances and their mixtures with inorganics of atmospheric importance. *Environ. Sci. Technol.* **37**, 5109–5115.

Chan, M. N. and Chan, C. K. 2005. Mass transfer effects in hygroscopic measurements of aerosol particles. *Atmos. Chem. Phys.* **5**, 2703–2712.

Chen, L. Y., Jeng, F. T., Chen, C. C. and Hsiao, T. C. 2003. Hygroscopic behaviour of atmospheric aerosol in Taipei. *Atmos. Environ.* **37**, 2069–2075.

Choi, M. Y. and Chan, C. K. 2002a. Continuous measurements of the water activities of aqueous droplets of water-soluble organic compounds. *J. Phys. Chem. A* **106**, 4566–4572.

Choi, M. Y. and Chan, C. K. 2002b. The effects of organic species on the hygroscopic behaviours of inorganic aerosols. *Environ. Sci. Technol.* **36**, 2422–2428.

Chuang, P. Y. 2003. Measurement of the timescale of hygroscopic growth for atmospheric aerosols. *J. Geophys. Res.-Atmos.* **108**, 4282, doi:4210.1029/2002JD002757.

Chylek, P. and Wong, J. G. D. 1998. Erroneous use of the modified Kohler equation in cloud and aerosol physics applications. *J. Atmos. Sci.* **55**, 1473–1477.

Clegg, S. L. and Simonson, J. M. 2001. A BET model of the thermodynamics of aqueous multicomponent solutions at extreme concentration. *J. Chem. Thermodyn.* **33**, 1457–1472.

Clegg, S. L., Seinfeld, J. H. and Edney, E. O. 2003. Thermodynamic modelling of aqueous aerosols containing electrolytes and dissolved organic compounds. II: an extended Zdanovskii-Stokes-Robinson approach. *J. Aerosol. Sci.* **34**, 667–690.

Cocker, D. R., Whitlock, N. E., Flagan, R. C. and Seinfeld, J. H. 2001. Hygroscopic properties of Pasadena, California aerosol. *Aerosol. Sci. Tech.* **35**, 637–647.

Cohen, M. D., Flagan, R. C. and Seinfeld, J. H. 1987a. Studies of concentrated electrolyte solutions using the electrodynamic balance. 2: water activities for mixed-electrolyte solutions. *J. Phys. Chem.* **91**, 4575–4582.

Cohen, M. D., Flagan, R. C. and Seinfeld, J. H. 1987b. Studies of concentrated electrolyte-solutions using the electrodynamic balance. 2: water activities for mixed-electrolyte solutions. *J. Phys. Chem.-Us.* **91**, 4575–4582.

Cohen, M. D., Flagan, R. C. and Seinfeld, J. H. 1987c. Studies of concentrated electrolyte-solutions using the electrodynamic balance. 1: water activities for single-electrolyte solutions. *J. Phys. Chem.-Us.* **91**, 4563–4574.

Cruz, C. N. and Pandis, S. N. 2000. Deliquescence and hygroscopic growth of mixed inorganic-organic atmospheric aerosol. *Environ. Sci. Technol.* **34**, 4313–4319.

Cubison, M. J., Coe, H. and Gysel, M. 2005. A modified hygroscopic tandem DMA and a data retrieval method based on optimal estimation. *J. Aerosol. Sci.* **36**, 846–865.

Cubison, M. J., Alfarra, M. R., Allan, J., Bower, K. N., Coe, H. and co-authors. 2006. The characterisation of pollution aerosol in a changing photochemical environment. *Atmos. Chem. Phys.* **6**, 5573–5588.

Dick, W. D., Saxena, P. and McMurry, P. H. 2000. Estimation of water uptake by organic compounds in submicron aerosols measured during the Southeastern Aerosol and Visibility Study. *J. Geophys. Res.-Atmos.* **105**, 1471–1479.

Dusek, U., Covert, D. S., Wiedensohler, A., Neususs, C., Weise, D. and co-authors. 2003. Cloud condensation nuclei spectra derived from size distributions and hygroscopic properties of the aerosol in coastal south-west Portugal during ACE-2. *Tellus* **55B**, 35–53.

Ehn, M., Petaja, T., Aufmhoff, H., Aalto, P., Hameri, K. and co-authors. 2007. Hygroscopic properties of ultrafine aerosol particles in the boreal forest: diurnal variation, solubility and the influence of sulphuric acid. *Atmos. Chem. Phys.* **7**, 211–222.

Facchini, M. C., Mircea, M., Fuzzi, S. and Charlson, R. J. 1999. Cloud albedo enhancement by surface-active organic solutes in growing droplets. *Nature* **401**, 257–259.

Ferron, G. A., Karg, E., Busch, B. and Heyder, J. 2005. Ambient particles at an urban, semi-urban and rural site in Central Europe: hygroscopic properties. *Atmos. Environ.* **39**, 343–352.

Finlayson-Pitts, B. J. and Hemminger, J. C. 2000. Physical chemistry of airborne sea salt particles and their components. *J. Phys. Chem. A* **49**, 11463–11477.

Gasparini, R., Li, R. J., Collins, D. R., Ferrare, R. A. and Brackett, V. G. 2006. Application of aerosol hygroscopicity measured at the Atmospheric Radiation Measurement Program's Southern Great Plains site to examine composition and evolution. *J. Geophys. Res.-Atmos.* **111**, D05S12, doi:10.1029/2004JD005448.

Ghosal, S. and Hemminger, J. C. 1999. Effect of water on the HNO_3 pressure dependence of the reaction between gas-phase HNO_3 and NaCl surfaces. *J. Phys. Chem. A* **103**, 4777–4781.

Grose, M., Sakurai, H., Savstrom, J., Stolzenburg, M. R., Watts, W. F. and co-authors. 2006. Chemical and physical properties of ultrafine diesel exhaust particles sampled downstream of a catalytic trap. *Environ. Sci. Technol.* **40**, 5502–5507.

Gysel, M., Weingartner, E. and Baltensperger, U. 2002. Hygroscopicity of aerosol particles at low temperatures. 2: theoretical and experimental hygroscopic properties of laboratory generated aerosols. *Environ. Sci. Technol.* **36**, 63–68.

Gysel, M., Weingartner, E., Nyeki, S., Paulsen, D., Baltensperger, U. and co-authors. 2004. Hygroscopic properties of water-soluble matter and humic-like organics in atmospheric fine aerosol. *Atmos. Chem. Phys.* **4**, 35–50.

Gysel, M., Crosier, J., Topping, D. O., Whitehead, J. D., Bower, K. N. and co-authors. 2007. Closure study between chemical composition and hygroscopic growth of aerosol particles during TORCH2. *Atmos. Chem. Phys.* **7**, 6131–6144.

Hameri, K., Vakeva, M., Hansson, H. C. and Laaksonen, A. 2000. Hygroscopic growth of ultrafine ammonium sulphate aerosol measured using an ultrafine tandem differential mobility analyzer. *J. Geophys. Res.-Atmos.* **105**, 22231–22242.

Hameri, K., Laaksonen, A., Vakeva, M. and Suni, T. 2001a. Hygroscopic growth of ultrafine sodium chloride particles. *J. Geophys. Res.-Atmos.* **106**, 20749–20757.

Hameri, K., Vakeva, M., Aalto, P. P., Kulmala, M., Swietlicki, E. and co-authors. 2001b. Hygroscopic and CCN properties of aerosol particles in boreal forests. *Tellus* **53B**, 359–379.

Hameri, K., Charlson, R. and Hansson, H. C. 2002. Hygroscopic properties of mixed ammonium sulfate and carboxylic acids particles. *Aiche. J.* **48**, 1309–1316.

Hansson, H. C., Rood, M. J., Koloutsou-Vakakis, S., Hameri, K., Orsini, D. and co-authors. 1998. NaCl aerosol particle hygroscopicity dependence on mixing with organic compounds. *J. Atmos. Chem.* **31**, 321–346.

Hartz, K. E. H., Rosenorn, T., Ferchak, S. R., Raymond, T. M., Bilde, M. and co-authors. 2005. Cloud condensation nuclei activation of monoterpene and sesquiterpene secondary organic aerosol. *J. Geophys. Res.-Atmos.* **110**, D14208, doi:14210.11029/12004JD005754.

Hennig, T., Massling, A., Brechtel, F. J. and Wiedensohler, A. 2005. A tandem DMA for highly temperature-stabilized hygroscopic particle growth measurements between 90% and 98% relative humidity. *J. Aerosol. Sci.* **36**, 1210–1223.

Jacobson, M. Z. 1999. *Fundamentals of Atmospheric Modelling*. Cambridge University Press, Cambridge, United Kingdom.

Johnson, G., Ristovski, Z. and Morawska, L. 2004a. Application of the VH-TDMA technique to coastal ambient aerosols. *Geophys. Res. Lett.* **31**, L16105, doi:16110.11029/12004GL020126.

Johnson, G. R., Ristovski, Z. and Morawska, L. 2004b. Method for measuring the hygroscopic behaviour of lower volatility fractions in an internally mixed aerosol. *J. Aerosol. Sci.* **35**, 443–455.

Johnson, G. R., Ristovski, Z. D., D'Anna, B. and Morawska, L. 2005. Hygroscopic behaviour of partially volatilized coastal marine aerosols using the volatilization and humidification tandem differential mobility analyzer technique. *J. Geophys. Res.-Atmos.* **110**, D20203, doi:20210.21029/22004JD005657.

Joutsensaari, J., Vaattovaara, P., Vesterinen, M., Hameri, K. and Laaksonen, A. 2001. A novel tandem differential mobility analyzer with organic vapour treatment of aerosol particles. *Atmos. Chem. Phys.* **1**, 51–60.

Joutsensaari, J., Toivonen, T., Vaattovaara, P., Vesterinen, M., Vepsalainen, J. and co-authors. 2004. Time-resolved growth behaviour of acid aerosols in ethanol vapour with a tandem-DMA technique. *J. Aerosol. Sci.* **35**, 851–867.

Kaku, K. C., Hegg, D. A., Covert, D. S., Santarpia, J. L., Jonsson, H. and co-authors. 2006. Organics in the Northeastern Pacific and their impacts on aerosol hygroscopicity in the subsaturated and supersaturated regimes. *Atmos. Chem. Phys.* **6**, 4101–4115.

Kanakidou, M., Seinfeld, J. H., Pandis, S. N., Barnes, I., Dentener, F. J. and co-authors. 2005. Organic aerosol and global climate modelling: a review. *Atmos. Chem. Phys.* **5**, 1053–1123.

Kandler, K. and Schutz, L. 2007. Climatology of the average water-soluble volume fraction of atmospheric aerosol. *Atmos. Res.* **83**, 77–92.

Kerminen, V. M. 1997. The effects of particle chemical character and atmospheric processes on particle hygroscopic properties. *J. Aerosol. Sci.* **28**, 121–132.

Kerminen, V. M., Lihavainen, H., Komppula, M., Viisanen, Y. and Kulmala, M. 2005. Direct observational evidence linking atmospheric aerosol formation and cloud droplet activation. *Geophys. Res. Lett.* **32**, L14803, doi:14810.11029/12005GL023130.

Khvorostyanov, V. I. a. C. 2007. Refinements to the Köhlers theory of aerosol equilibrium radii, size spectra, and droplet activation: effects of humidity and insoluble fraction. *J. Geophys. Res.* **112**, D05206.

Koehler, K. A., Kreidenweis, S. M., DeMott, P. J., Prenni, A. J., Carrico, C. M. and co-authors. 2006. Water activity and activation diameters from hygroscopicity data—Part II: application to organic species. *Atmos. Chem. Phys.* **6**, 795–809.

Köhler, H. 1936. The nucleaus in and the growth of atmospheric droplets. *Trans. Faraday Soc.* **32**, 1152–1161.

Kokkola, H., Sorjamaa, R., Peraniemi, A., Raatikainen, T. and Laaksonen, A. 2006. Cloud formation of particles containing humic-like substances. *Geophys. Res. Lett.* **33**, L10816, doi:10810.11029/12006GL026107.

Kreidenweis, S. M., Koehler, K., DeMott, P. J., Prenni, A. J., Carrico, C. and co-authors. 2005. Water activity and activation diameters from hygroscopicity data—Part I: theory and application to inorganic salts. *Atmos. Chem. Phys.* **5**, 1357–1370.

Kulmala, M., Dal Maso, M., Makela, J. M., Pirjola, L., Vakeva, M. and co-authors. 2001. On the formation, growth and composition of nucleation mode particles. *Tellus* **53B**, 479–490.

Kulmala, M., Vehkamaki, H., Petajda, T., Dal Maso, M., Lauri, A. and co-authors. 2004. Formation and growth rates of ultrafine atmospheric particles: a review of observations. *J. Aerosol. Sci.* **35**, 143–176.

Leck, C. and Bigg, E. K. 2005. Source and evolution of the marine aerosol—A new perspective. *Geophys. Res. Lett.* **32**, L19803, doi:19810.11029/12005GL023651.

Li, Z. D., Williams, A. L. and Rood, M. J. 1998. Influence of soluble surfactant properties on the activation of aerosol particles containing inorganic solute. *J. Atmos. Sci.* **55**, 1859–1866.

Liu, B. Y. H., Pui, D. Y. H., Whitby, K. T., Kittelson, D. B., Kousaka, Y. and co-authors. 1978. Aerosol mobility chromatograph—new detector for sulphuric-acid aerosols. *Atmos. Environ.* **12**, 99–104.

Londahl, J., Massling, A., Pagels, J., Swietlicki, E., Vaclavik, E. and co-authors. 2007. Size-resolved respiratory-tract deposition of fine and ultrafine hydrophobic and hygroscopic aerosol particles during rest and exercise. *Inhal Toxicol* **19**, 109–116.

Malm, W. C. and Kreidenweis, S. M. 1997. The effects of models of aerosol hygroscopicity on the apportionment of extinction. *Atmos. Environ.* **31**, 1965–1976.

Marcolli, C., Luo, B. P. and Peter, T. 2004. Mixing of the organic aerosol fractions: liquids as the thermodynamically stable phases. *J. Phys. Chem. A* **108**, 2216–2224.

Marcolli, C. and Krieger, U. K. 2006. Phase changes during hygroscopic cycles of mixed organic/inorganic model systems of tropospheric aerosols. *J. Phys. Chem. A* **110**, 1881–1893.

Martensson, E. M., Nilsson, E. D., de Leeuw, G., Cohen, L. H. and Hansson, H. C. 2003. Laboratory simulations and parameterization of the primary marine aerosol production. *J. Geophys. Res.-Atmos.* **108**, 4297, doi:4210.1029/2002JD002263.

Massling, A., Wiedensohler, A., Busch, B., Neususs, C., Quinn, P. and co-authors. 2003. Hygroscopic properties of different aerosol types over the Atlantic and Indian Oceans. *Atmos. Chem. Phys.* **3**, 1377–1397.

Massling, A., Stock, M. and Wiedensohler, A. 2005. Diurnal, weekly, and seasonal variation of hygroscopic properties of submicrometer urban aerosol particles. *Atmos. Environ.* **39**, 3911–3922.

Massling, A. L. S., Wiedensohler, A. and Covert, D. 2006. Hygroscopic growth of sub-micrometer and one-micrometer aerosol particles measured during ACE-Asia. *Atmos. Chem. Phys.-Discuss.* **6**, 12268–12300.

McFiggans, G., Alfarra, M. R., Allan, J., Bower, K., Coe, H. and co-authors. 2005. Simplification of the representation of the organic component of atmospheric particulates. *Faraday Discuss* **130**, 341–362.

McFiggans, G., Artaxo, P., Baltensperger, U., Coe, H., Facchini, M. C. and co-authors. 2006. The effect of physical and chemical aerosol properties on warm cloud droplet activation. *Atmos. Chem. Phys.* **6**, 2593–2649.

McMurry, P. H., Takano, H. and Anderson, G. R. 1983. Study of the ammonia (Gas) sulfuric-acid (aerosol) reaction-rate. *Environ. Sci. Technol.* **17**, 347–352.

McMurry, P. H. and Stolzenburg, M. R. 1989. On the sensitivity of particle-size to relative-humidity for Los-Angeles aerosols. *Atmos. Environ.* **23**, 497–507.

McMurry, P. H., Litchy, M., Huang, P. F., Cai, X. P., Turpin, B. J. and co-authors. 1996. Elemental composition and morphology of individual particles separated by size and hygroscopicity with the TDMA. *Atmos. Environ.* **30**, 101–108.

Mikhailov, E., Vlasenko, S., Niessner, R. and Poschl, U. 2004. Interaction of aerosol particles composed of protein and salts with water vapour: hygroscopic growth and microstructural rearrangement. *Atmos. Chem. Phys.* **4**, 323–350.

Ming, Y. and Russell, L. M. 2001. Predicted hygroscopic growth of sea salt aerosol. *J. Geophys. Res.-Atmos.* **106**, 28259–28274.

Ming, Y. and Russell, L. M. 2002. Thermodynamic equilibrium of organic-electrolyte mixtures in aerosol particles. *Aiche. J.* **48**, 1331–1348.

Mirabel, P., Reiss, H. and Bowles, R. K. 2000. A theory for the deliquescence of small particles. *J Chem Phys* **113**, 8200–8205.

Mircea, M., Facchini, M. C., Decesari, S., Cavalli, F., Emblico, L. and co-authors. 2005. Importance of the organic aerosol fraction for modeling aerosol hygroscopic growth and activation: a case study in the Amazon Basin. *Atmos. Chem. Phys.* **5**, 3111–3126.

Nilsson, E. 2007. Hygroscopic growth factors of nebulized bulk sea water samples. Private Communication, Division of Nuclear Physics, Lund University, PO Box 118, S-22100 Lund, Sweden.

Nilsson, E. D., Rannik, U., Swietlicki, E., Leck, C., Aalto, P. P. and co-authors. 2001. Turbulent aerosol fluxes over the Arctic Ocean. 2: wind-driven sources from the sea. *J. Geophys. Res.-Atmos.* **106**, 32139–32154.

O'Dowd, C. D., Aalto, P., Hameri, K., Kulmala, M. and Hoffmann, T. 2002. Aerosol formation—atmospheric particles from organic vapours. *Nature* **416**, 497–498.

O'Dowd, C. D., Facchini, M. C., Cavalli, F., Ceburnis, D., Mircea, M. and co-authors. 2004. Biogenically driven organic contribution to marine aerosol. *Nature* **431**, 676–680.

Peng, C. G. and Chan, C. K. 2001. The water cycles of water-soluble organic salts of atmospheric importance. *Atmos. Environ.* **35**, 1183–1192.

Petaja, T., Kerminen, V. M., Hameri, K., Vaattovaara, P., Joutsensaari, J. and co-authors. 2005. Effects of SO_2 oxidation on ambient aerosol growth in water and ethanol vapours. *Atmos. Chem. Phys.* **5**, 767–779.

Petaja, T., Kerminen, V. M., Dal Maso, M., Junninen, H., Koponen, I. K. and co-authors. 2007. Sub-micron atmospheric aerosols in the surroundings of Marseille and Athens: physical characterization and new particle formation. *Atmos. Chem. Phys.* **7**, 2705–2720.

Pitchford, M. L. and McMurry, P. H. 1994. Relationship between measured water-vapour growth and chemistry of atmospheric aerosol for Grand-Canyon, Arizona, in winter 1990. *Atmos. Environ.* **28**, 827–839.

Quinn, P. K., Anderson, T. L., Dlugi, R., Heintzenberg, J., von Hoyningen-Huene, W. and co-authors. 1996. The state of closure in tropospheric aerosol climate research: a review and future research needs. *Contri. Atmos. Phys.* **69**, 547–577.

Quinn, P. K. and Bates, T. S. 2005. Regional aerosol properties: comparisons of boundary layer measurements from ACE 1, ACE 2, aerosols99, INDOEX, ACE asia, TARFOX, and NEAQS. *J. Geophys. Res.-Atmos.* **110**, D14202, doi:14210.11029/12004JD004755.

Rader, D. J. and McMurry, P. H. 1986. Application of the Tandem Differential Mobility Analyzer to Studies of Droplet Growth or Evaporation. *J. Aerosol Sci.* **17**, 771–787.

Randall, D. A., Wood, R. A., Bony, S., Colman, R., Fichefet, T. and co-authors. 2007. *Contribution of Working Group I to the Fourth Assessment Report of the Intergovernmental Panel on Climate Change—Climate Models and their Evaluation*. Cambridge University Press, Cambridge, UK.

Reilly, P. J. and Wood, R. H. 1969. Prediction of properties of mixed electrolytes from measurements on common ion mixtures. *J. Phys. Chem.-Us.* **73**, 4292-&.

Rissler, J., Swietlicki, E., Zhou, J., Roberts, G., Andreae, M. O. and co-authors. 2004. Physical properties of the sub-micrometer aerosol over the Amazon rain forest during the wet-to-dry season transition—comparison of modeled and measured CCN concentrations. *Atmos. Chem. Phys.* **4**, 2119–2143.

Rissler, J., Pagels, J., Swietlicki, E., Wierzbicka, A., Strand, M. and co-authors. 2005. Hygroscopic behaviour of aerosol particles emitted from biomass fired grate boilers. *Aerosol. Sci. Tech.* **39**, 919–930.

Rissler, J., Vestin, A., Swietlicki, E., Fisch, G., Zhou, J. and co-authors. 2006. Size distribution and hygroscopic properties of aerosol particles from dry-season biomass burning in Amazonia. *Atmos. Chem. Phys.* **6**, 471–491.

Rissler, J., Svenningsson, B., Swietlicki, E., Bilde, M., Mircea, M. and co-authors. 2008. Critical supersaturations from hygroscopic growth—a laboratory evaluation of a CCN model. *Atmos. Chem. Phys.*, to be submitted.

Rissman, T. A., Varutbangkul, V., Surratt, J. D., Topping, D. O., McFiggans, G. and co-authors. 2007. Cloud condensation nucleus (CCN) behaviour of organic aerosol particles generated by atomization of water and methanol solutions. *Atmos. Chem. Phys.* **7**, 2949–2971.

Rodgers, C. 1976. Retrieval of atmospheric temperature and composition from remote measurements of thermal radiation. *Rev. Geophys.* **14**, 609–624.

Rodgers, C. 1990. Characterization and error analysis of profiles retrieved from remote sounding measurements. *J. Geophys. Res.* **95**, 5587–5595.

Russell, L. M. and Ming, Y. 2002. Deliquescence of small particles. *J. Chem. Phys.* **116**, 311–321.

Saathoff, H., Naumann, K. H., Schnaiter, M., Schock, W., Mohler, O. and co-authors. 2003. Coating of soot and $(NH_4)_2SO_4$ particles by ozonolysis products of alpha-pinene. *J. Aerosol. Sci.* **34**, 1297–1321.

Sakurai, H., Fink, M. A., McMurry, P. H., Mauldin, L., Moore, K. F. and co-authors. 2005. Hygroscopicity and volatility of 4–10 nm particles during summertime atmospheric nucleation events in urban Atlanta. *J. Geophys. Res.-Atmos.* **110**, D22S04, doi:10.1029/2005JD005918.

Santarpia, J. L., Li, R. J. and Collins, D. R. 2004. Direct measurement of the hydration state of ambient aerosol populations. *J. Geophys. Res.-Atmos.* **109**, D18209, doi:18210.11029/12004JD004653.

Saxena, P., Hildemann, L. M., McMurry, P. H. and Seinfeld, J. H. 1995. Organics alter hygroscopic behaviour of atmospheric particles. *J. Geophys. Res.-Atmos.* **100**, 18755–18770.

Sekigawa, K. 1983. Estimation of the volume fraction of water soluble material in submicron aerosols in the atmosphere. *J. Meteor. Soc. Japan* **61**, 359–366.

Shulman, M. L., Jacobson, M. C., Charlson, R. J., Synovec, R. E. and Young, T. E. 1996. Dissolution behaviour and surface tension effects of organic compounds in nucleating cloud droplets (vol 23, pg 277, 1996). *Geophys. Res. Lett.* **23**, 603–603.

Sjogren, S., Gysel, M., Weingartner, E., Alfarra, M. R., Duplissy, J. and co-authors. 2007a. Hygroscopicity of the submicrometer aerosol at the high-alpine site Jungfraujoch, 3580 m a.s.l., Switzerland. *Atmos. Chem. Phys. Discuss.* **7**, 13699–13732.

Sjogren, S., Gysel, M., Weingartner, E., Baltensperger, U., Cubison, M. J. and co-authors. 2007b. Hygroscopic growth and water uptake kinetics of two-phase aerosol particles consisting of ammonium sulphate, adipic and humic acid mixtures. *J. Aerosol. Sci.* **38**, 157–171.

Sorjamaa, R., Svenningsson, B., Raatikainen, T., Henning, S., Bilde, M. and co-authors. 2004. The role of surfactants in Kohler theory reconsidered. *Atmos. Chem. Phys.* **4**, 2107–2117.

Stokes, R. H. and Robinson, R. A. 1966 Interactions in aqueous nonelectrolyte solutions. I: solute-solvent equilibria. *J. Phys. Chem.-Us.* **70**, 2126–2130.

Stolzenburg, M. R. and McMurry, P. H. 1988. *TDMAFIT User's Manual*. Particle Technology Laboratory, Department of Mechanical Engineering, U of Minnesota, Minneapolis, MN 55455.

Stratmann, F., Orsini, D. and Kauffeldt, T. 1997. Inversion algorithm for TDMA measurements. *J. Aerosol. Sci.* **28**, S701–S702.

Svenningsson, B., Hansson, H. C., Wiedensohler, A., Noone, K., Ogren, J. and co-authors. 1994. Hygroscopic growth of aerosol-particles and its influence on nucleation scavenging in-cloud—experimental results from Kleiner-Feldberg. *J. Atmos. Chem.* **19**, 129–152.

Svenningsson, B., Hansson, H. C., Martinsson, B., Wiedensohler, A., Swietlicki, E. and co-authors. 1997. Cloud droplet nucleation scavenging in relation to the size and hygroscopic behaviour of aerosol particles. *Atmos. Environ.* **31**, 2463–2475.

Svenningsson, B., Rissler, J., Swietlicki, E., Mircea, M., Bilde, M. and co-authors. 2006a. Hygroscopic growth and critical supersaturations for mixed aerosol particles of inorganic and organic compounds of atmospheric relevance. *Atm. Chem. Phys.* **6**, 1937–1952.

Svenningsson, B., Rissler, J., Swietlicki, E., Mircea, M., Bilde, M. and co-authors. 2006b. Hygroscopic growth and critical supersaturations for mixed aerosol particles of inorganic and organic compounds of atmospheric relevance. *Atmos. Chem. Phys.* **6**, 1937–1952.

Svenningsson, B., Bilde, M., Rissler, J. and Swietlicki, E. 2007. What about water uptake by mixtures of four of the most important atmospheric aerosol ions: NH_4^+, Na+, SO_4^{2-}, and Cl^-? In: *European Aerosol Conference*, Salzburg, Austria.

Svenningsson, I. B., Hansson, H. C., Wiedensohler, A., Ogren, J. A., Noone, K. J. and co-authors. 1992. Hygroscopic growth of aerosol-particles in the Po Valley. *Tellus* **44B**, 556–569.

Swietlicki, E., Zhou, J. C., Berg, O. H., Martinsson, B. G., Frank, G. and co-authors. 1999. A closure study of sub-micrometer aerosol particle hygroscopic behaviour. *Atmos. Res.* **50**, 205–240.

Swietlicki, E., Zhou, J. C., Covert, D. S., Hameri, K., Busch, B. and co-authors. 2000. Hygroscopic properties of aerosol particles in the northeastern Atlantic during ACE-2. *Tellus* **52B**, 201–227.

Tang, I. N. and Munkelwitz, H. R. 1994. Water activities, densities, and refractive indices of aqueous sulfates and sodium nitrate droplets of atmospheric importance. *J. Geophys. Res.* **99**(D9), 18801–18808.

Tang, I. N. 1997. Thermodynamic and optical properties of mixed-salt aerosols of atmospheric importance. *J. Geophys. Res.-Atmos.* **102**, 1883–1893.

Tang, I. N., Tridico, A. C. and Fung, K. H. 1997. Thermodynamic and optical properties of sea salt aerosols. *J. Geophys. Res.-Atmos.* **102**, 23269–23275.

Tomlinson, J. M., Li, R. J. and Collins, D. R. 2007. Physical and chemical properties of the aerosol within the southeastern Pacific marine boundary layer. *J. Geophys. Res.-Atmos.* **112**, D12211, doi:12210.11029/12006JD007771.

Topping, D. O., McFiggans, G. B. and Coe, H. 2005a. A curved multi-component aerosol hygroscopicity model framework: Part 1—Inorganic compounds. *Atmos. Chem. Phys.* **5**, 1205–1222.

Topping, D. O., McFiggans, G. B. and Coe, H. 2005b. A curved multi-component aerosol hygroscopicity model framework: Part 2—Including organic compounds. *Atmos. Chem. Phys.* **5**, 1223–1242.

Topping, D. O., McFiggans, G. B., Kiss, G., Varga, Z., Facchini, M. C. and co-authors. 2007. Surface tensions of multi-component mixed inorganic/organic aqueous systems of atmospheric significance: measurements, model predictions and importance for cloud activation predictions. *Atmos. Chem. Phys.* **7**, 2371–2398.

Tunved, P., Hansson, H. C., Kerminen, V. M., Strom, J., Dal Maso, M. and co-authors. 2006a. High natural aerosol loading over boreal forests. *Science* **312**, 261–263.

Tunved, P., Korhonen, H., Strom, J., Hansson, H. C., Lehtinen, K. E. J. and co-authors. 2006b. Is nucleation capable of explaining observed aerosol integral number increase during southerly transport over Scandinavia? *Tellus* **58B**, 129–140.

Vakeva, M., Hameri, K., Puhakka, T., Nilsson, E. D., Hohti, H. and co-authors. 2000. Effects of meteorological processes on aerosol particle size distribution in an urban background area. *J. Geophys. Res.-Atmos.* **105**, 9807–9821.

Vakeva, M., Hameri, K. and Aalto, P. P. 2002a. Hygroscopic properties of nucleation mode and Aitken mode particles during nucleation bursts and in background air. *J. Geophys. Res.-Atmos.* **107**, 8104, doi:8110.1029/2000JD000176.

Vakeva, M., Kulmala, M., Stratmann, F. and Hameri, K. 2002b. Field measurements of hygroscopic properties and state of mixing of nucleation mode particles. *Atmos. Chem. Phys.* **2**, 55–66.

Van Dingenen, R., Putaud, J. P., Martins-Dos Santos, S. and Raes, F. 2005. Physical aerosol properties and their relation to air mass origin at Monte Cimone (Italy) during the first MINATROC campaign. *Atmos. Chem. Phys.* **5**, 2203–2226.

Vestin, A., Rissler, J., Swietlicki, E., Frank, G. P. and Andreae, M. O. 2007. Cloud-nucleating properties of the Amazonian biomass burning aerosol: cloud condensation nuclei measurements and modeling. *J. Geophys. Res.-Atmos.* **112**, D14201, doi:14210.11029/12006JD008104.

Virkkula, A., Van Dingenen, R., Raes, F. and Hjorth, J. 1999. Hygroscopic properties of aerosol formed by oxidation of limonene, alpha-pinene, and beta-pinene. *J. Geophys. Res.-Atmos.* **104**, 3569–3579.

Voutilainen, A., Stratmann, F. and Kaipio, J. P. 2000. A non-homogeneous regularization method for the estimation of narrow aerosol size distributions. *J. Aerosol. Sci.* **31**, 1433–1445.

Wang, S. C. and Flagan, R. C. 1990. Scanning electrical mobility spectrometer. *Aerosol Sci. Tech.* **13**, 230–240.

Weingartner, E., Burtscher, H. and Baltensperger, U. 1997. Hygroscopic properties of carbon and diesel soot particles. *Atmos. Environ.* **31**, 2311–2327.

Weingartner, E., Gysel, M. and Baltensperger, U. 2002. Hygroscopicity of aerosol particles at low temperatures. 1. New low-temperature H-TDMA instrument: setup and first applications. *Environ. Sci. Technol.* **36**, 55–62.

Weis, D. D. and Ewing, G. E. 1999. Water content and morphology of sodium chloride aerosol particles. *J. Geophys. Res.-Atmos.* **104**, 21275–21285.

Wexler, A. S. and Clegg, S. L. 2002. Atmospheric aerosol models for systems including the ions H^+, NH_4^+, Na^+, SO_4^{2-}, NO_3^-,Cl^-, Br^-, and H_2O. *J. Geophys. Res.-Atmos.* **107**, 4207, doi:4210.1029/2001JD000451.

Zdanovskii, A. 1948. New methods for calculating solubilities of electrolytes in multicomponent systems. *Zhur. Fiz. Khim.* **22**, 1475–1485.

Zhang, X. Q., McMurry, P. H., Hering, S. V. and Casuccio, G. S. 1993. Mixing characteristics and water-content of submicron aerosols measured in Los-Angeles and at the Grand-Canyon. *Atmos. Environ. Part A-General Topics* **27**, 1593–1607.

Zhou, J. C., Swietlicki, E., Berg, O. H., Aalto, P. P., Hameri, K. and co-authors. 2001. Hygroscopic properties of aerosol particles over the central Arctic Ocean during summer. *J. Geophys. Res.-Atmos.* **106**, 32111–32123.

Zhou, J. C., Swietlicki, E., Hansson, H. C. and Artaxo, P. 2002. Submicrometer aerosol particle size distribution and hygroscopic growth measured in the Amazon rain forest during the wet season. *J. Geophys. Res.-Atmos.* **107**, 8055, doi:8010.1029/2000JD000203.